VOLUMETRIC MRI ANALYSIS OF THALAMIC STROKE PATIENTS

by

Pınar Özel

BS, Electronics Engineering, Erciyes University, 2007

Submitted to the Institute of Biomedical Engineering
in partial fulfillment of the requirements
for the degree of
Master of Science
in
Biomedical Engineering

Boğaziçi University
2011

VOLUMETRIC MRI ANALYSIS OF THALAMIC STROKE PATIENTS

APPROVED BY:

Prof. Dr. Ahmet Ademoğlu .....
(Thesis Advisor)

Doç. Dr. Burak Güçlü .....

Prof. Dr. Sadık Kara .....

DATE OF APPROVAL: 31 March 2011

ACKNOWLEDGMENTS

First of all, I would like to thank my supervisor Prof. Dr. Ahmet Ademoğlu and Research Assistant Adil Deniz Duru for their help and encouragement throughout my graduate study.

I wish to thank the Neurology Department in Faculty at the Medicine in Istanbul University for providing me MRI data. Especially, I must express my gratitude to Dr. Ferda Ilgen Uslu for answering my questions sincerely.

In addition, I would like to thank my dear friends Aysel Fışgın, Taliha Paşaoğlu, Betül Polat, Elif Kubat, Fatma Şimşek and Aslıhan Dinçer for their unlimited encouragement.

And also, I want to state my thanks to Caner Gümüş for his help in Latex environment.

Finally, I would like to thank my parents, my elder sister and my brother for their invaluable support and encouragement. Without their support, I could never make it this far.

ABSTRACT

VOLUMETRIC MRI ANALYSIS OF THALAMIC STROKE PATIENTS

The thalamic pain syndrome is a weakly deduced phenomenon that develops as a complication of a small stroke in the thalamus. Because this syndrome results in many different physiological disturbances, it is critical to understand its physiological basis to diagnose and to treat it. It is important to determine the whole volume of the lesion and to label it with reference to an anatomical atlas in order to identify the stroke region more accurately. In this thesis, we develop a software tool to help the neuroradiologists interpret the stroke region more accurately by estimating its volume and identifying its anatomical label. To reduce the anatomical variability, the first step consists of spatial registration and normalization of brain images. This is achieved using the procedure implemented in the Statistical Parametric Mapping (SPM) package in Matlab. Normalized MR images are used to identify the lesions in the brain, to calculate its volume and to label it in a graphical user environment. Three types of neuropsychological tests *i.e.* are Mini-Mental State Examination (MMSE), Frontal Behavioral Inventory (FBI), Beck Depression Inventory (BDI) are evaluated in estimating their correlations with the total volume of selected regions. Neuroradiologists can potentially benefit from the software to diagnose and to treat the thalamic stroke patients. Furthermore, such a platform may help the clinicans to interact with each other distantly by exchanging more objective information about the clinical neuroanatomical assessment of their patients. Additionally, correlation analysis of neuropsychological tests and stroke volume in the Talairach atlas plays a role for the neuropsychological and neuroanatomical data fusion for a better assessment.

Keywords: Thalamic syndrome, registration, normalization, structural MRI, Talairach atlas, Neuropsychologic tests, MMSE, FBI, BDI.

ÖZET

TALAMİK İNME HASTALARIN VOLUMETRİK MRG ANALİZİ

Talamus içindeki küçük bir inmenin komplikasyonu sonrası oluşun Talamik inme sendromu, az bilinen bir sendromdur. Bu sendrom farklı fizyolojik problemlerle de sonuçlanacağından, bu problemleri anlamak, hastalığı teşhis etmek ve daha doğru bir şekilde tedavi etmek açısından önemlidir. Dolayısıyla, inme olan bölgeyi daha iyi yorumlamak için lezyon bölgesinin tüm hacmini belirlemek ve bir anatomik atlasa göre etiketlemek oldukça önem taşır. Bu tezde, nöroradyologların inmeyi daha doğru yorumlamasına yardımcı olmak amacıyla, lezyon bölgesinin anatomik etiketini bulan ve lezyon hacmini tahmin eden bir yazılım aracı geliştirildi. Anatomik değişkenliği azaltmak için ilk aşama Matlab üzerinde çalışan SPM5 yazılımı kullanılarak, alınan beyin görüntülerinin uzaysal olarak çakıştırma ve olağanlaştırma aşamasıydı. Talairach Atlasına dayalı ara-yüz vasıtasıyla, beyindeki lezyonlu bölgeyi seçip, lezyonun hacminin hesaplanmasında ve lezyonun tam olarak nerede olduğunun işaretlenmesinde elde edilen normalize edilmiş MR görüntüleri kullanıldı. Mini-Mental Durum Muayenesi (MMSE), Frontal Davranış Envanteri (FBI), Beck Depresyon Envanteri (BDI) olmak üzere üç tip nöropsikometrik test bu çalışmada değerlendirildi. Nöropsikomerik testler ile Talairach atlasına göre seçilmiş lezyon bölgelerinin hacimleri arasında korelasyon analizi yapıldı ve sonuçlar sunuldu. Nöroradyologlar, talamik inme hastalarını teşhis etmek ve tedavilerine yardımcı olmak amacıyla bu yazılımdan yararlanabilir. Ayrıca, böyle bir platform klinisyenlerin hastaları üzerinde nöroanatomik değerlendirmesi hakkında uzaktan birbirleriyle bilgi alışverişine yardımcı olabilir. Buna ek olarak, nöropsikometrik testler ile atlasa göre seçilen bölgelerin hacimleri arasında yapılan korelasyon analizinin sonuçları bu verilerin birlikte yorumlanmasında rol oynayabilir.

Anahtar Sözcükler: Talamik inme, registrasyon, normalizasyon, anatomik MRG, Talairach atlas, Nöropsikometrik test, MMSE, FBI, BDI.

TABLE OF CONTENTS

LIST OF FIGURES

LIST OF TABLES

LIST OF ABBREVIATIONS

CVA	Cerebrovascular Accident
FLAIR	Fluid-attenuated Inversion Recover
DWI	Diffusion-Weighted Imaging
CT	Computerized Tomography
SPECT	Single Photon Emission Computed Tomography
fMRI	Functional Magnetic Resonance Imaging
f-FLAIR	Fast Fluid-attenuated Inversion Recovery
GUI	Graphical User Interface
PWI	Perfusion-Weighted Imaging
MRI	Magnetic Resonance Imaging
PET	Positron Emission Tomography
TD	Talairach Daemon
CDFI	Color Doppler Flow Imaging
TCCS	Transcranial Color-Coded Duplex Sonography
PW	Pulse Wave
VOTL	Volume Occupancy Talairach Labels
CNA	Cerefy Neuroradiology Atlas
MNI	Montreal Neurological Institute
MMSE	Mini–Mental State Examination
NIF	Neuroscience Information Framework
NITRC	Neuroimaging Informatics Tools and Resources Clearinghouse
IATR	Internet Analysis Tools Registry
IBVD	The Internet Brain Volume Database
FBI	Frontal Behavioral Inventory
BDI	Beck Depression Inventory
SPM	Statistical Parametric Mapping
MD	Medial Dorsal
Pul	Pulvinar

VL	Ventral Lateral
VPL	Ventroposterolateral
IML	Internal Meduller Lamina
VPM	Ventroposteromedian
Pum	Medial Pulvinar
Pua	Anterior Pulvinar
MGN	Medial Geniculat Nucleus
LGN	Lateral Geniculat Nucleus
RN	Reticular Nucleus

1. INTRODUCTION

1.1 Motivation and objectives

A stroke (sometimes called a cerebrovascular accident (CVA)) occurs when a blood clot blocks an artery or a blood vessel breaks, interrupting blood flow to an area of the brain. When either of this findings happens, brain cells begin to die. Thalamic syndrome is a type of stroke that can be related to insufficient blood supply from the posterior cerebral artery. It is an uncommon neurological disorder in which the body becomes hypersensitive to pain due to injury in the thalamus. Because thalamic stroke is of vital importance, more studies are needed to be conducted to evaluate its physiological effects on patients.

Spatial illustration of the thalamic lesions is important, for the fact that some of the dissociated thalamic nuclei only have a volume of a few cubic milimeters, and every nucleus has its own forward and reverse feeding features. By means of these features, the lesions show complicated images although thalamus exists in a very small area. Because of the recent improvements in neuroimaging, it is now possible to localize the thalamic lesions, nucleus dissociation and volume. By this way, the clinical data can be more finely correlated with the imaging and prognosis findings. The animal experiments that have been made over a century has also proven that many anatomical relations are arranged by means of these nuclei in the thalamus [1].

In this thesis, we develop a software tool to help the neuroradiologists to interpret the stroke more accurately by identifying and labelling lesion. The selected volume is estimated and its anatomical substructures are identified by labelling them with reference to the atlas. The percentage volume of each substructure is also estimated to generate a 'fingerprint' of the stroke in a neuroanatomical sense.

In this study, structural lesions of 43 patients, that are diagnosed by acute

isolated thalamic infarction problem, are localized by an expert neurologist using this software tool; the correlation between the percentage volumes and the clinical and neuropsychological tests are estimated.

Chapter 2 begins with an overview of the Thalamic Pain Syndrome and its diagnostic and Neuropsychological Tests. Then anatomic atlases and labelling methods are introduced and some studies using different anatomic atlas and labelling methods are reviewed. Chapter 3 describes the proposed method and its implementation for anatomical labelling. Chapter 4 gives the results. Chapter 5 discusses the results and offers some recommendations for future work.

2. BACKGROUND

2.1 Thalamic pain syndrome and its diagnostic tests

According to a definition which is devised by the World Health Organization in the 1970s, stroke is a 'neurological lack of cerebrovascular reason that continue more than 24 hours or is stopped by death within 24 hours' [2]. The 24-hour border separates stroke from transient ischemic attack, which is a related syndrome of stroke symptoms that resolve totally within 24 hours [3]. Stroke is the most usual life-intimidating neurologic disease and is the third leading reason of death in the United States, after heart disease and cancer [4]. Although stroke is more often disabling than lethal, stroke mortality for 2005 was 143,579 [5]. In the elder people, the segment of population where most stroke occurs, it is also a major source of disability [2]. The American Heart Association estimated there are more than 6 million people in the United States today have survived a stroke [5].

A stroke (sometimes called a cerebrovascular accident (CVA)) occurs when a blood clot blocks an artery (a blood vessel that carries blood from the heart to the body) or a blood vessel (a tube through which the blood moves through the body) breaks, interrupting blood flow to an area of the brain. When either of these things happens, brain cells begin to die [4]. When brain cells die during a stroke, abilities controlled by that area of the brain are lost. These abilities include speech, movement and memory. How a stroke patient is affected depends on where the stroke occurs in the brain and how much the brain is damaged [5]. Strokes can be divided into two chief classes: ischemic and hemorrhagic [6]. Ischemic strokes are those that occur because of interruption of the blood supply, however hemorrhagic strokes - whose types are intracerebral hemorrhage or subarachnoid hemorrhage - stems from the fact that rupture of a blood vessel or an abnormal vascular structure. 87% of strokes are caused by ischemia, and the remainder by hemorrhage. Among the stroke types caused by ischemia, approximately 1.1% of them are isolated thalamic infarct [7] and the thalamus is one of

the most affected area for intracerebral hemorrhages [8]. At the beginning of this century Dejerine and Roussy presented a comprehensive description of thalamic syndrome [4]. Thereafter, in 1925 Lhermitte and in 1930 Baudouin *et. al.* made significant contributions by explaining the characteristics of thalamic hemorrhage [9, 10, 11]. Fisher showed the importance of language defect and ocular motility disturbances in thalamic hemorrhage [6]. According to these definitions, thalamic syndrome (or Dejerine Roussy syndrome) is a disease that can be in a relation with insufficient blood supply from the posterior cerebral artery. It is an uncommon neurological disorder in which the body becomes hypersensitive to pain due to injury to the thalamus [8].

2.1.1 The anatomy and location

The thalamus, which is a diencephalic structure, has a nuclei that represents an entrance for input and output to and from the cerebral cortex. It takes, modifies, and relays information from somatomotor reticular formation, major afferent and limbic system pathways. The thalamus is supplied by four arterial systems, three derived from the vertebrobasilar system (paramedian thalamo - subthalamic, thalamo-geniculate, and posterior choroidal arteries) and one derived from the posterior communicating artery (polar artery). Vascular lesions in each of these territories give rise to distinct clinical syndromes. The thalamus performs as a central processing center for sensory information flowing toward the brain from the rest of the body. Sensory knowledge such as touch, pressure, heat, cold, and pain circulates along nerves from all parts of the body into the spinal cord, where it travels upward along privated paths toward the brain. As all of the different sensory tracts go into the brain through the brainstem, they come together upon the thalamus, where the multitude of sensations are processed and integrated . And then the thalamus relays them to suitable areas of the brain where the information is used or brought into the individual's conscious awareness [7, 11, 12].

The lateral part of thalamus is covered by myelinated axons and forms the External Medullar Lamina (EML) and separates the thalamus from capsula interna. Inside the EML, the reticular nucleus, which is a cluster of cells, is located [13]. The grey

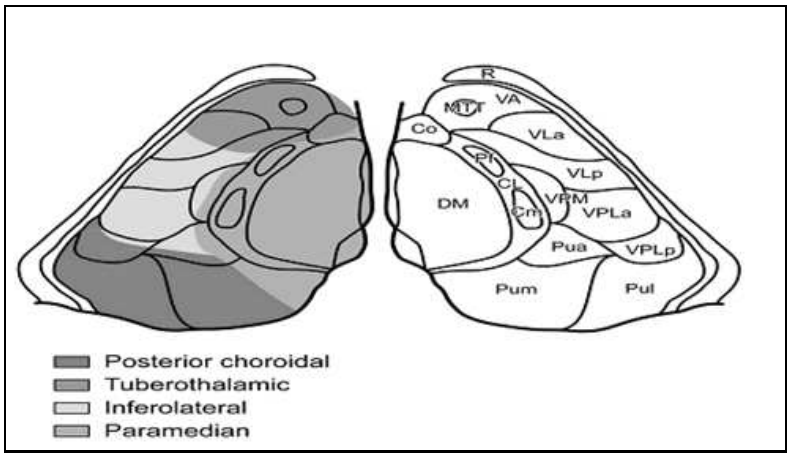

Figure 2.1 The nuclei of thalamus.

matter forming the thalamus is separated into main parts by means of white matter lamina named Internal Medullar Lamina (IML), which passes through the middle of the grey matter and can be seen by naked eye [14, 15]. In this lamina, some of the fibers from and to the nuclei of the thalamus and small nuclei are located. This lamina, that seperates thalamus into two in sagittal plane, divides into two planes in upper-front part. Between the planes of IML, anterior nuclei are located together with the medial nuclei inside and lateral group nuclei outside parts [13]. As a result, the thalamus is separated into 4 parts anatomically and functionally by IML and EML: inferolateral, paramedian, anterior and posterior [16]. There is a fifth region inside the thalamus, called intralaminar nuclei, surrounded by these lamina [15]. In Figure 2.1, the most noticeable nucleci of thalamus are shown. In Table 2.1, the abbreviations for the nuclei of Thalamus shown in Figure 2.1 is presented.

Table 2.1
The abbreviations for the some nuclei of Thalamus

MD	Medial Dorsal
Pul	Pulvinar
VL	Ventral Lateral
VPL	Ventroposterolateral
IML	Internal meduller lamina
VPM	Ventroposteromedian
Pum	Medial pulvinar
Pua	Anterior pulvinar
MGN	Medial geniculate nucleus
LGN	Lateral geniculate nucleus
RN	Reticular nucleus

2.1.2 The diagnostic tests of thalamic stroke

Recent advances in the field of radiology exhibited precise diagnoses and made possible the examination of clinical characteristics and pathology without autopsy study. The clinical and radiological features and prognosis of thalamic stroke have been documented in more recent studies. Different case reports have concentrated on separate deficits in thalamic syndrome [8]. Different diagnostic tests examine how the brain looks, works and obtains its blood supply and these tests can be classified into three categories.

- Imaging tests give a picture of the brain - MRI, CT, PET.
- Electrical tests inscribe the electrical impulses of the brain - EEG, MEG.
- Blood flow tests exhibit any problem that may lead to changes in blood flow to the brain - Ultrasound [17].

Much of the current comprehension of the function and anatomy of thalamus is derived from imaging tests known as in vivo neuroimaging. The anatomic precision of MRI, including diffusion-weighted imaging, fluid-attenuated inversion recover (FLAIR) MRI, T2 weighted , T1 weighted gives a significant advance over CT [12]. The advent of other MRI techniques such as perfusion-weighted (PWI) has also revolutionized diagnostic image in stroke. Another form of imaging is T2* weighted imaging that tends to emphasize blood products and is useful in detecting small amounts of hemorrhage [4].

Diffusion-weighted imaging has the possibility to improve the early anatomic diagnosis of stroke and hence in the evolvement and implementation of early stroke interventions [12]. DWI with echo-planar imaging seems significantly beneficial to identify a physiological parameter that is susceptible to ischemia changes before the conventional MRI is performed. However its potential function in the quantitative study of human stroke patho-physiology and therapeutics is needed to be further investigated [18]. DWI seems to be more susceptible than CT for the early detection of ischemic stroke in selected patients.

Fast fluid-attenuated inversion recovery (f-FLAIR) is more susceptible than conventional or fast spin echo T2 weighted magnetic resonance imaging (MRI) for lesions in the brain of patients with ischemic, inflammatory or demyelinating disease of the CNS [19]. Functional imaging methods have also a significant role to diagnose stroke types; especially Xenon computed tomography cerebral blood flow imaging is acquiring acceptance and has now been supplemented by a single photon emission computed tomography (SPECT). Both show local and distant functional effects after stroke, and some have demonstrated effects of resting flows remote from the site of infarction. When it is applied quickly after stroke, and the deficit in local flow may be evident before the tissue signal changes appear on CT or MR scan [4]. As to positron emission tomography (PET), it remains the best method for demonstrating viable tissue in carotid occlusive disease and has been able to demonstrate remote effects of infarction, some spread over wide areas some explained as diaschisis [4]. Especially, for the assessment of stable stroke, SPECT and PET may be helpful.

EEG has been widely used for 30 years to detect acute cerebral ischemia. In that EEG morphology, frequencies, and amplitudes have a physiological connection with cerebral blood flow [20, 21]. Studies from intra-operative EEG monitoring and animal models have shown that EEG changes occur within 5 minutes of acute cerebral ischemia [22, 23].

A variety of noninvasive ultrasound techniques have been developed during recent years for the detection of cerebrovascular disease. Some of these, such as continuous wave and pulse wave(PW) devices are used for the examination of the intra and extracranial brain-supplying arteries. In addition to these systems color doppler flow imaging (CDFI) gives color-coded, real time information about intravascular blood flow superimposed on the gray scale image of vessel anatomy. Low frequency, high energy PW Doppler systems are utilized for transcranial doppler examinations. Transcranial color-coded duplex sonography (TCCS) is a rapidly improving technique for estimation of cerebrovascular disease that provides a quick enhancing area of ultrasound imaging. Additionally, contrast-enhanced TCCS gives precise examinations in two thirds of patients with ischemic cerebrovascular disease [4].

2.2 Anatomic atlases and labelling methods

Neurodegenerative disorders, psychiatric disorders and healthy aging are often related with structural changes in the brain. These changes can bring about modifications in the imaging properties of brain tissue, as well as changes in morphometric properties of brain structures. Morphometric alterations may contain variations in the volume or shape of subcortical regions, in addition to alterations in the thickness, area, and folding pattern of the cortex. While surface based analysis that depends on models and the positions and orientation of the cortical ribbon can provide an accurate estimation of cortical variability, volumetric techniques are necessary to discern alterations in non-cortical structures. For example, changes in ventricular or hippocampal volume are frequently associated with a variety of diseases [24].

Furthermore, while finding structural changes or comparing functions across brains, it is prevalent to label the gross anatomy of brain image data and to compare the structures or functions that lie within anatomically labeled regions. Due to the fact that brains differ in their anatomy, it would be plausible to refer to the anatomy of many brains when labelling an individual subject's brain image. For this purpose, a wide variety of labelling methods and brain atlases -which explain and list rudimentary spatial features of brain structure using traditional nomenclature- in neuroimaging today have been designed with particular anatomical bases, and with varying degrees of granularity in their delineations.

The first stereotactic brain atlases in printed form, as an example of Talairach et al. and Schaltenbrand and Bailey were assembled in the 1950s [25, 26]. Approximately, two decades later, brain atlases in electronic formats were ready for use in the clinical setting. In 1977, Atlas for Stereotaxy of the Human Brain was presented by Schaltenbrand and Wahrenin [27]. By the late 1990s, electronic brain atlases had been worthy of conventional in stereotactic functional neurosurgery. This made an example by the extensive use of the 1988 Talairach atlas by the human brain mapping community. Prevalent usage of Talairach coordinates [28] encouraged the progression of the Brain Map database that encrypts and asks the locations of functional and anatomical neuroimaging results using these coordinates [29]. The Talairach Daemon (TD) system [30] broadens this idea by supplying easy Internet access to a 3-dimensional (3-D) database of brain labels obtained by Talairach coordinates. The Talairach labels database uses a volume-filling hierarchical naming scheme to organize labels for brain structures ranging from hemispheres to cytoarchitectural regions [31]. This scheme is reflected in the database name, Volume Occupancy Talairach Labels (VOTL).

Beginning in the late 1990s, a new-generation brain atlas which is known as population-based probabilistic brain atlas (or probabilistic map) has been under construction. It provides the explanation about the structural and functional anatomy of any given position in the stereotaxic standard space. The probabilistic maps are applicable in making analysis the structure and function of the brain that is complex

and individually variable [32, 33]. The location of the activated foci in the functional brain mapping research could be labeled without difficulty and reproducibly using the probabilistic maps [34].

The Cerefy electronic brain atlas database containing an extended and enhanced electronic version of Talairach and Tournoux and other atlases was presented by Nowinski et al. [35, 36]. Cerefy Neuroradiology Atlas (CNA), which is a java-based tool, allows the user to load anatomical and functional neuroimage data, correlate them, and label in interactive way with subcortical structures and cortical areas. The CNA is appropriate for a rapid atlas-assisted analysis of neuroimages [37].

As an alternative to reference brain of the Talairach and Tournoux atlas, MNI structural atlas which is more representative of population is offered. fMRI or PET data are often normalized to the templates provided by the Montreal Neurological Institute (MNI). The most widely used MNI templates are a single subject template and a group template produced from 152 individual brains, both of which are adjusted to the Talairach Atlas [38, 39]. A single subject's structural image was hand segmented, and the labels were then procreated to more than 50 subjects' structural images using nonlinear registration. Each labelled brain outcome was then transmuted into MNI152 space using affine registration, before averaging segmentations across subjects to produce the final probability images. Although these templates are roughly based on the Talairach space, they do not match the Talairach brain in size and shape [40].

Apart from these mentioned ones, a variety of different types have been presented. Talairach and Tournoux and Ono et al. put forward, in the beginning of 1990s, Referentially Oriented Cerebral MRI Anatomy: Atlas of Stereotaxic Anatomical Correlations for Gray and White Matter and Atlas of the Cerebral Sulci respectively [41, 42]. More recently, Centre for Morphometric Analysis in Harvard proposed Harvard-Oxford cortical and subcortical structural atlas [43]. A probabilistic atlas called Jülich histological (cyto- and myelo-architectonic) atlas created by averaging multi-subject post-mortem cyto- and myelo-architectonic segmentations, performed by the team of Zilles and Amunts at the Research Center Jülich and provided by Simon Eickhoff

[44, 45, 46]. Similarly, an atlas called probabilistic cerebellar atlas with 28 anatomical structural regions, provided by Joern Diedrichsen, Institute of Cognitive Neuroscience, UCL and Narender Ramnani, Cognitive Neuroscience Laboratory, Royal Holloway is supposed [47]. The LONI Probabilistic Brain Atlas (LPBA40), a series of maps of brain anatomic regions is presented by Shattuck DW in 2008 [48]. The SRI24 atlas, a new standard reference system of normal human brain anatomy was produced using template-free population registration of high-resolution magnetic resonance images acquired at 3T in a group of 24 normal control subjects [49].

Oxford thalamic connectivity atlas and a probabilistic atlas of 7 sub-thalamic regions, segmented according to their white-matter connectivity to cortical areas are provided by Heidi Johansen-Berg and Timothy Behrens [50, 51]. This connectivity atlas provides probability of anatomical junction from points in the thalamus to each of 7 cortical zones. These probabilities are estimated using probabilistic diffusion tractography in multiple subjects [52].

There are also visualization tools for other aspects of the neuroimaging process, and one example is Nielsen et al.'s Brede Toolbox [53]. The Brede Toolbox now includes its own database results from neuroimaging in addition to analysis and visualization purposes for a variety of tasks [54, 55] – the Brede Database by starting out as a program for handling and visualization of data from the Brain Map database [56]. Its principal functions are handling, analyzing and visualizing data from functional neuroimaging experiments, not the original data but rather the summary images (e.g., statistical parametric images) and location data in stereotaxic space. It consists of numerous general purpose analysis algorithms (e.g., independent component analysis and non-negative matrix factorization, text and link analysis, probabilistic modeling of activation foci, visualization of multiple foci, volumes, surfaces, slices or points (Talairach coordinates) and/or surfaces in a 3-dimensional model language) [57].

The Pick Atlas software toolbox presents a technique for producing ROI masks depending on the Talairach Daemon database. The atlases contain Brodmann area, Lobar, Hemisphere, Anatomic Label (gyral anatomy) and Tissue Type. The software

was planned so as to be added the extra atlases directly, containing non-human atlases. Each type of atlas in a shared imaging space should be in one subdirectory [58, 59]

SPM Anatomy toolbox which is MATLAB dependent toolbox for the SPM software package is capable of integrating probabilistic cytoarchitectonic maps and findings of functional imaging studies. The toolbox contains the functionality for the construction of summary maps uniting likelihood of various cortical areas by deciding the most reasonable determination of each voxel to one of these areas. Its principal feature is to present numerous assessments explaining the degree of matching between architectonic areas and functional foci [44].

Rather than using a single (average or probabilistic) atlas, Mindboggle software operates multiple atlases in a database autonomously to label the cortical voxels of a subject brain image, and for each voxel selects the greater label alloted by the different atlases. Their aim here, in fact, is to examine the impacts of using distinctive labelling schemes and variable numbers of atlases on labelling accuracy and on the numbers of labels alloted per voxel [60].

Nowinski et al. developed a software called BAFI to perform a rapid and user friendly atlas-assisted analysis of functional images. The BAFI includes a fully color coded, labeled, expanded, and improved Talairach-Tournoux brain atlas in axial, coronal, and sagittal orientations, as well as Brodmann areas and gyri in axial orientation. It is capable of loading one anatomical and a matching functional data set (in TIFF and AVW-Analyze file formats), interactively place the Talairach landmarks in 3D space, and automatically warp the data to the atlas by utilizing the Talairach proportional grid system transformation. The precision of warping can be, afterwards, fine adjusted in interactive way. The anatomical image, functional image, and atlas cover combined together are revealed as a single image with atlas-anatomy and anatomy-function blending controlled autonomously. The data warped to the atlas can be labeled efficiently with the names of subcortical structures, gyri, and Brodmann areas. Additionally, triplanar display and navigation, in which one plane from the data and the other two from the atlas, makes easy comprehension of 3D relationships [61].

The plentifulness of tools for imaging as well as for other point of view of the neuroimaging procedure has generated a concern in causing overviews for these tools, and now there occur numerous Web-based directories: Neuroscience Database Gateway (NDG) [62], Neuroscience Information Framework (NIF) [63], Neuroimaging Informatics Tools and Resources Clearinghouse (NITRC) [64], I Do Imaging and Internet Analysis Tools Registry (IATR), see also [65, 66].

A great many tools are available for efficient neuroimaging visualization across the Internet. Often these tools are dependent on a client–server model with the client carring out the visualization and graphical user interface in Java. Among these tools, JIV is that renders multiple volume data by orthogonal slice views performed as a Java applet [67]. iiV executes a resembling purpose [68], and MindSeer can also transform in 3D distantly [69]. NeuroTerrain implements 3D visualization and has presented its use in connection with a Mouse atlas [70]. The Talairach Applet renders a digital performance of the Talairach Atlas and fuses it with neuroanatomical labelling of coordinates via the Talairach Daemon depicted by [30]. Additionally, connected to the BrainMap database the Java client- program Sleuth plots 3D points in orthogonal 2D slices based on user query to the BrainMap server [71]. The Internet Brain Volume Database (IBVD) records published values for brain region volumes across variables such as gender and diagnosis [72].

In this study, we preferred to use the the Talairach and Tournoux atlas because of its prevalent use. And also, the most consistent structure was ascertained as the thalamus in the studies for determination of consistency Talairach and Tournoux atlas. While the consistency is 85.7%, the inconsistency is 5.4% without any error tolarance in the thalamus, when the error tolerance is increased to 3mm, this ratio 94.6% and 0.7% is determined respectively [13, 30].

2.3 Neuropsychological tests

Neuropsychological tests are particularly formed assignments used to measure a psychological function known to be connected to a particular brain structure or pathway. They commonly require the organized administration of manifestly defined procedures in a formal environment. Neuropsychological tests are normally managed to a single person working with an examiner in a quiet office environment, free from distractions. It can be claimed that neuropsychological tests sometimes suggest an estimate of a person's top level of perceptive performance. Most neuropsychological tests in present use are established on traditional psychometric theory and they are a central part of the process of managing neuropsychological estimation [73].

Neurophysiologists use methodically confirmed objective tests to appraise brain functions. While neurological examination and CT, MRI, EEG and PET scans search the structural, physical, and metabolic condition of the brain, the neuropsychological examination is the only way to conventionally evaluate brain function.

Neuropsychological tests review the range of mental processes from simple motor performance to complex reasoning and problem solving. In nearly whole objective tests, quantitative results are compared with some normative standard, including data from group of non-brain injured persons and group of persons with various kinds of brain injury. If the norms are dependent on age and educational achievement, valid comparison can be made between an individual's performance and that of people in known diagnostic categories as well as people who do not have a diagnosis of brain injury [73].

In this study, we benefit from three types of neuropsychological tests acquired from the thalamic stroke investigation in which the same thalamic stroke patients are participated in. The utilized neuropsychologic tests in this study are Mini–Mental State Examination (MMSE), Frontal Behavioral Inventory (FBI), Beck Depression Inventory (BDI). Following sections give a brief information about them.

2.3.1 Mini-Mental State Examination (MMSE)

The Mini–Mental State Examination (MMSE) introduced by Folstein et al. in 1975 [74] is a short 30-point questionnaire test that is used to sift for cognitive impairment. It is used to estimate the severity of perceptive deterioration at a given point as time passes and to follow the course of cognitive alterations in an individual over time, thus making it an effective way to document an individual's response to treatment. The MMSE test contains simple questions and problems in numerous areas: the time and place of the test, repeating lists of words, arithmetic, language use and comprehension, and basic motor skills.

Any score greater than or equal to 25 points (out of 30) is productively intact (normal). Below this, scores can point out serious ($\leq$ 9 points), moderate (10-20 points) or mild (21-24 points) [75]. The raw score may also need to be corrected for educational attendance and age [76]. Low to very low scores correlate nearly with the presence of dementia, although other mental disorders can also cause abnormal findings on MMSE testing.

2.3.2 Frontal Behavioral Inventory (FBI)

The Frontal Behavioral Inventory (FBI) is a 24 item, quantifiable questionnaire directed to the caregiver. The inventory requires a reliable observer, unlike some depression or other behavioural inventories directly administered with the patients. It is intended for a face to face interview style. Interview is about (20-30) minutes, depending on the extent and severity of symptoms and the caregivers verbal capacity. At times caregivers unload a large number of symptoms and disturbing behaviours in a cathartic fashion. Skilled interviewers can usually keep the answers within a reasonable time frame [77, 78].

The FBI test is divided into two categories : Negativity Behavioral Materials : Apathy, Aspontaneity, Indifference\Emotional Flatness, Inflexibility, Disorganiza-

tion, Inattention, Personal Neglect, Loss of Insight, Logopenia, Aphasia and Verbal Apraxia, Comprehension (Semantic) deficit. Disinhibition Excessive or Abnormal Behavioral Materials: Perseveration, Obsessions (Stereotypy), Hoarding, Inappropriateness , Excessive jocularity, Poor Judgement and Impulsivity, Restlessness\Roaming , Irritability, Aggression, Hyperorality\food fads, Hypersexuality, Utilization Behaviour, Incontinence. During scoring of frotal inventory scale, the score is given as '0=non-existent, 1=mild, 2=moderate, 3=severe' and the total score taken from FBI test changes between 0 and 72 [13].

2.3.3 Beck Depression Inventory (BDI)

The Beck Depression Inventory produced by Dr. Aaron T. Beck is a 21 question multiple choice self-report inventory and one of the most known used instruments for measuring the severity of depression [79, 80].

In its current version the questionnaire is planned for individuals aged 13 and over, and is comprised of items relating to symptoms of depression such as hopelessness and irritability, cognitions such as guilt or feelings of being punished, as well as physical symptoms such as fatigue, weight loss, and lack of interest in sex [81]. When the test is scored, a value of 0 to 3 is allotted for each answer and then the total score is compared to a key to decide the depression's severity. The standard cut-offs are as follows: 0-9 indicates minimal depression, 10-18 indicates mild depression, 19-29 points out moderate depression and 30-63 points out severe depression. Higher total scores signify more severe depressive symptoms [81].

There are three types of the BDI-the primary BDI, first published in 1961 and lag revised in 1978 as the BDI-1A, and the BDI-II, published in 1996. The BDI is extremely used as an estimation tool by health care professionals and researchers in a diversity of environment [82].

3. METHODOLOGY

3.1 Pre-Processing

In neuroimaging studies, it is significant to decease anatomical variability among subjects and to evaluate the image to a standard space. For this reason, the necessary steps consists of applying tools for spatial registration and normalization of brain images taken from different individuals. This can be achieved using, especially, the procedure performed in the Statistical Parametric Mapping package however, before touching on SPM package, it is considerably important to know how co-registration and normalization steps are applied to the image.

3.1.1 Registration

Registration is the establishing of a geometrical transformation that aligns points in one view of an object with corresponding points in another view of that object or another object and therefore, the process of transformation different sets of data into one coordinate system [83, 84].

One image is presumed to remain stationary, also known as the reference image, while the other image which is known as the source image is spatially transformed to match it. In order to transform the source to match the reference, it is important to settle a mapping from each voxel place in the reference to a corresponding place in the source. The source is then re-sampled at the new positions. The mapping can be considered as a function of a set of estimated transformation parameters. A rigid-body transformation in three dimensions is defined by six parameters: three translations and three rotations [85].

3.1.2 Normalization

Spatial normalization is more specifically an image registration technique. Human brains are different in size and shape, so one objective of spatial normalization is to deform human brain scans so that one location in one subject's brain scan matches to the same location in another subject's brain scan. Spatial normalization requires transforming all the subject's data to the same stereotactic space. In this process, each of the images are registered to the same template image by reducing the residual sum of squared differences between them. Respectively, in the implementation, the first step in spatially normalizing each image entangles corresponding the image by assessing the optimum 12-parameter affine transformation [86]. Unlike Registration where the images to be matched together are from the same subject zooms and shears are needed to register heads of different shapes and sizes. Prior knowledge of the variability of head sizes is contained within a Bayesian framework so as to enhance the robustness and accuracy of the method. The second part depicts nonlinear registration for amending gross differences in head shapes that cannot be responsible for by the affine normalization alone. The nonlinear warps are displayed by linear combinations of smooth discrete cosine transform basis functions [87].

The mathematical implementations of the registration and the normalization steps are given in [87, 85]. The details of these steps in SPM5 package are presented in Appendix A.

3.2 Graphical user interface and the Talairach atlas

3.2.1 Talairach atlas labelling scheme

It is becoming more widespread to label subject brain image data with a single or compound atlas depicting an average of multiple brain atlases. Since it was announced, the Talairach system is the most prevalent coordinate system in human brain mapping,

and the number of references to the Talairach-Tournoux atlas continues to expand in an exponential manner.

The 1988 Talairach-Tournoux atlas includes a set of high detail color tracings (coronal, axial, and sagittal slices) taken from MR images of a 60-year old right handed European female. A unique 3-D coordinate-based database composition was improved for setting brain labels. The center of the database is a 3-D image array covering the full extent of Talairach space at a resolution of 1-mm with x-y-z dimensions of 770x200x210 mm. Each 1-mm^3 voxel within this 3-D array embraces a pointer to a voxel record that gives information concerning labels for that voxel. Each voxel index includes pointers to labels. This system grants rapid indexed access to any label with in this space. More specifically, that is, the Talairach labels database, for brain structures ranging from hemispheres to cytoarchitectural regions, utilizes a volume-filling hierarchical naming scheme to arrange labels [30, 88]. This scheme is known as Volume Occupancy Talairach Labels (VOTL). The VOIs in the computerized 3-D Talairach atlas were systematized into five hierarchical levels: Hemisphere, Lobe, Gyrus, Tissue type, and Cell type. Regulations and methods were adopted for the VOTL labelling scheme to clearly explain borders for labeled brain structures [30, 88], and the entire brain volume fully labeled at each hierarchical level (Fig. 3.1). The regulations and methods for the VOTL labelling scheme are summarized below:

- Talairach level 1 (Hemisphere level) - Main structures (left, right cerebrum, cerebellum, brain stem, and so on)
- Talairach level 2 (Lobe level) - Lobes (temporal, frontal, parietal, posterior, occipital, limbic, anterior, midbrain, and so on)
- Talairach level 3 (Gyrus level) - Gyri (temporal, precentral, fusiform, thalamus, ventricles, and so on)
- Talairach level 4 (Tissue level) - Matter (white matter, gray matter, CSF)
- Talairach level 5 (Cell level) - Brodmann areas (areas 1-47, hippocampus putamen, and so on)

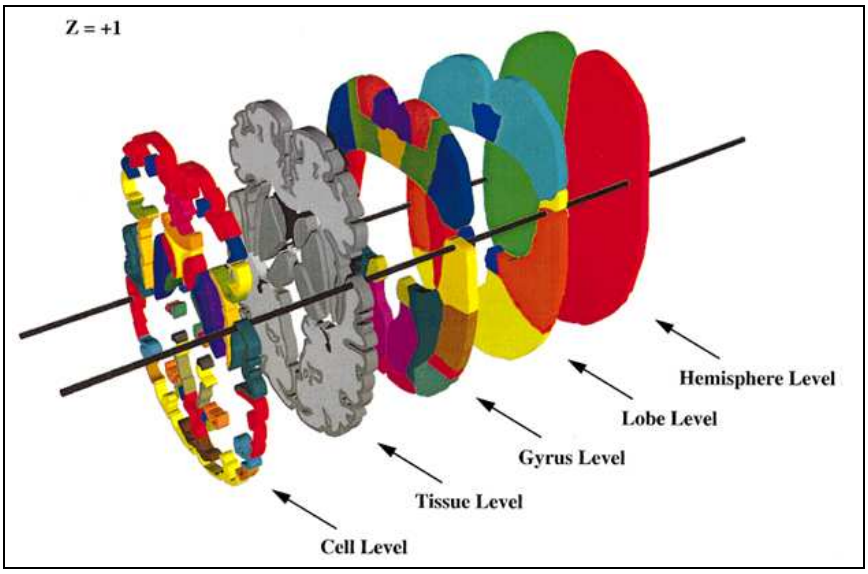

Figure 3.1 A typical set of 3-D data used to create the volume occupancy database around the z 5-11 level. Openings in lobe through cell levels were provided to emphasize the 3-D nature of data at each level

The Talairach coordinates allow researchers to easily identify subregions of the brain and measure their volume. It includes labels for 148 different substructures of the brain at various scales, along with a set of volumetric images of the labels(Fig. 3.2)

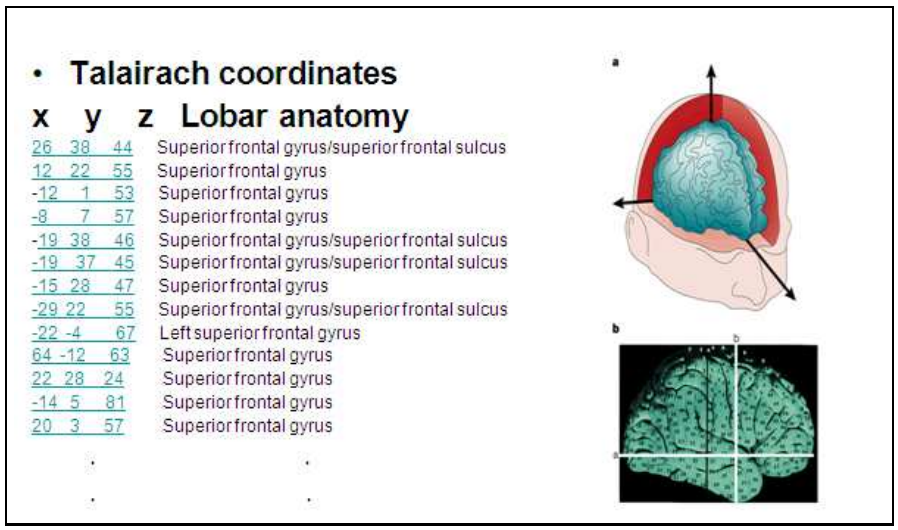

Figure 3.2 A part of Talairach atlas

3.2.2 Difference between the MNI templates and the Talairach brain

In order to utilize MR images in neuroimaging or brain mapping applications, it is necessary to adjust MR images according to a standard space and to match them to a standard image. For the sake of these purposes, two methods - registration and normalization respectively - are used. Registration is a process that MR images in a different coordinate system must be modified according to standard coordinate system. Normalization is to deform human brain scans so that one location in one subject's brain scan matches to the same location in another subject's brain scan because human brains are different in size and shape. SPM5 toolbox is used for both registration and normalization process. SPM96 and later versions use standard brains for its templates from the Montreal Neurological Institute (MNI). The MNI wanted to define a brain that was more representative of the population and defined a new standard brain by using a large series of MRI scans on normal controls. There are several MNI templates such as MNI305 brain, MNI152 brain. SPM99 and later versions use the MNI average of 152 scans. This means that the Talairach atlas is not precisely appropriate for understanding coordinates from SPM analyses, on the condition that the scans have been spatially normalized and registered to the SPM templates (that is generally the case). This can be a problem because there is no publicly known MNI atlas which clarifies Brodmann's areas on the MNI brain. However, there is attainable information on Brodmann's areas for the Talairach atlas.

In SPM analysis, the coordinates are in the Talairach system that $(0, 0, 0)$ is at the center of the anterior/posterior commissural (AC/PC) line. Actually, the center of the AC/PC line is not precisely at $(0, 0, 0)$ in the MNI brain, but approximately 4mm below. This stems from the fact that the Talairach atlas brain is a rather odd shape, and so, it is troublesome to correspond a standard brain to the atlas brain using an affine transform. It is obvious to say that the MNI brains are somewhat larger especially higher, deeper and longer than the Talairach brain.

The disagreements are not clear on axial slices, however, they are obvious on coronal sections. Figure 3.3 exhibits the MNI 152 average brain section from the SPM

templates, with the same slice of the Talairach atlas. As can be seen in Figure 3.3, the highest point of the brain is higher in MNI, and the temporal lobes are significantly lower and larger than those for the Talairach brain [89].

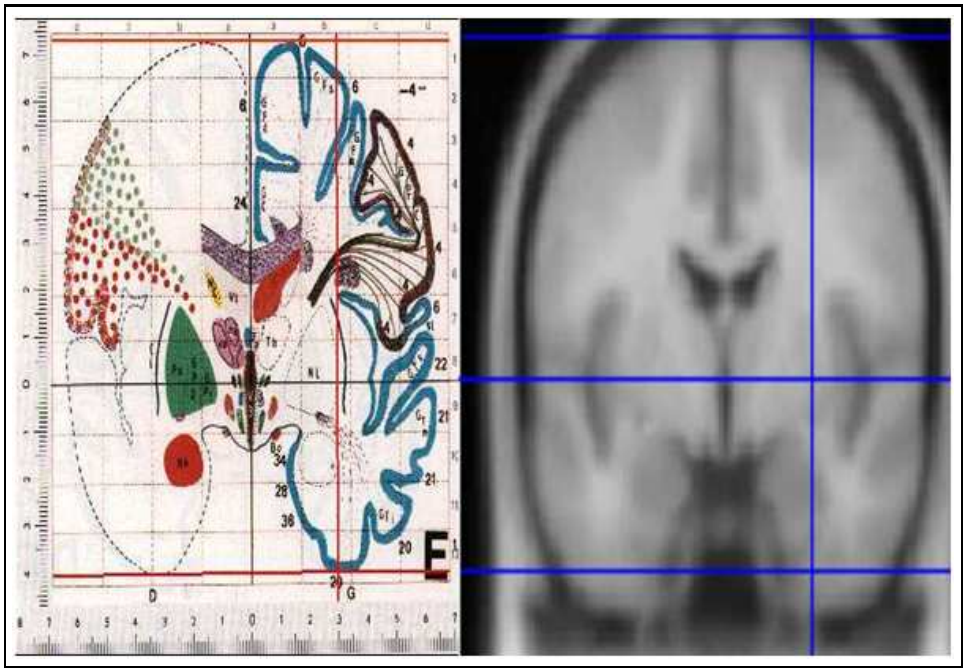

Figure 3.3 Differences between the Talairach brain and MNI templates

3.2.3 Converting between MNI and Talairach spaces

Previously, BrainMap has used the Brett transform to transform MNI coordinates to Talairach space (mni2tal.m). However, it has been recently switched to a new MNI space to Talairach space transform called 'icbm2tal.m'.

The results of Lancaster et al. [90] present that MNI/Talairach coordinate bias associated with reference frame (position and orientation) and scale (brain size) can be considerably lessened utilizing the best-fit 'icbm2tal' transform. This transform has been confirmed and shown to grant improved fit over the Brett 'mni2tal' transform. In SPM5 [91], we use these transformation formulas as 'tal2icbm_spm.m' and 'tal2icbm_other.m' respectively.

3.3 Implementation

The objective of the study is to identify the location of anatomical sites of the brain and to evaluate the corresponding total stroke region volume correspondingly. The development section can be divided into three subsections

- The procedure of MR data collection
- The application of registration and normalization to MR images
- The design of graphical user interface to select the stroke region on normalized magnetic resonance images.

3.3.1 General features of MRI data

T2 weighted anatomic MR images are acquired via 1.5 Tesla 'Philips Achieva' MR modality in the Department of Neurology at the Istanbul Faculty of Medicine in Istanbul University, from 43 patients diagnosed with isolated ischemic thalamic stroke following at least one and a half months after the stroke exists. In this study, the axial T2 MRI of patients are used. The general feature of T2 weighted MRI are KK: 3 mm, gap: 1 mm, FOV = AP (mm): 220, RL (mm): 182, FH (mm): 63; NSA: 4, section: 16, matrix: 244x512, TE (ms): 100, TR (ms): 3230.

3.3.2 The application of registration and normalization norms to MR images

In registration, two types of images, the reference and source images are utilized. The reference image is the image that is assumed to remain stationary (sometimes known as the target or template image), while the source image is moved to match it. In SPM5 package, the reference image is a type of image that conforms to the space defined by the ICBM, NIH P-20 project, which is approximated to the space described

in the atlas of Talairach and Tournoux (1988). In this study, 'avg152t2(T2.nii.1)' is preferred as the reference image.

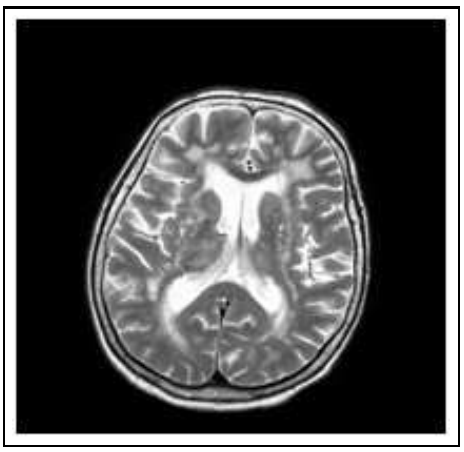

Figure 3.4 MR image of a patient diagnosed with isolated ischemic thalamic stroke.

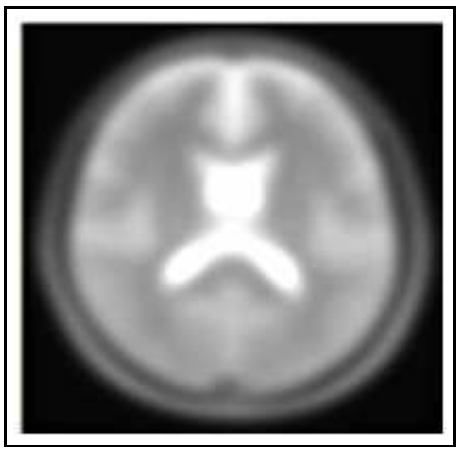

Figure 3.6 The template image used in SPM5.

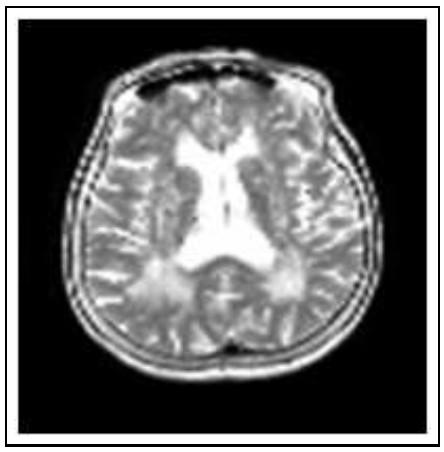

Figure 3.5 Registered MR image of the same patient diagnosed with isolated ischemic thalamic stroke.

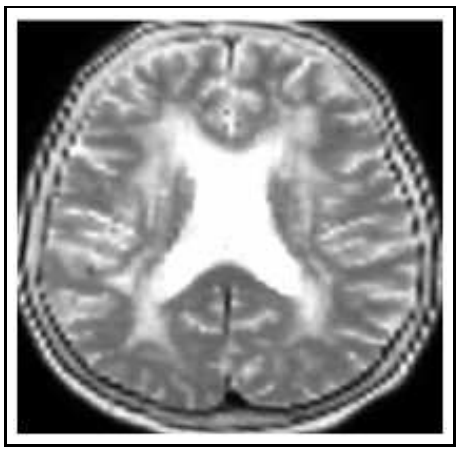

Figure 3.7 Spatially normalized MR image of the patient diagnosed with isolated ischemic thalamic stroke.

In Figures (3.4), (3.5), (3.6) and (3.7) , the raw MR image, the template image in SPM5 package, the registered MR image and the normalized MR image are presented, respectively.

3.3.3 Selection of the stroke region

In Figure 3.8, the graphical user interface for selection of region with lesion for a patient diagnosed with thalamic stroke is presented.

The axial cranial MRI investigation is performed for 43 patients identified with isolated thalamic infarct during the chronic period. During normalization procedure, the resolution of existing images is defined as 0.43mmx0.43mmx0.43mm in order to reduce the error in determining the stroke region.

The Talairach atlas which consists of 1105 different anatomic labels with a size of '141x172x110' (Figure 3.2), is used to determine the label of anatomic region.

After loading the normalized MR images to the GUI setup , regions with infarct were marked by an expert neurologist who followed up the thalamic stroke patients regularly at Istanbul University, Istanbul Medical School.

As can be seen in Figure 3.1 and Figure 3.2 (Talairach atlas labelling scheme), results are presented in five hierarchical levels. Brain voxel size is 0.43mmx0.43mmx0.43mm. Voxels with the same label are grouped and the percentage volume is computed. Hence, MR images of all patients are analyzed using the procedure.

The matlab script of the graphical user interface for selection of region with lesion is given in Appendix B.

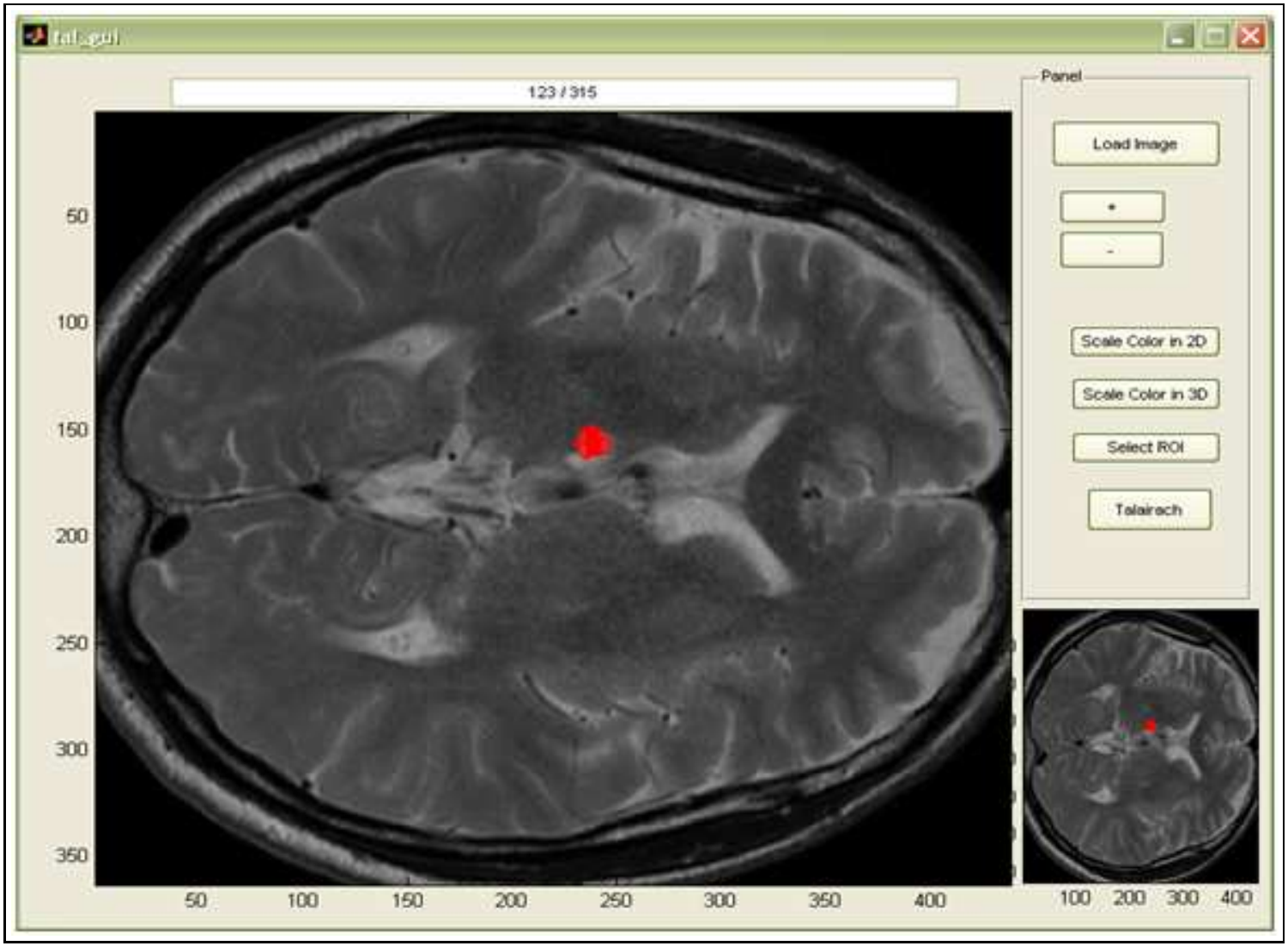

Figure 3.8 The Graphical user interface for selection of lesion region of the patient diagnosed with thalamic stroke. (The points with red colour denote to the region with lesion)

3.4 Correlation analysis

Correlation analysis is used to determine the extent to which changes in the value of an attribute are associated with changes in another attribute. The data for a correlation analysis consists of two input columns. Each column contains values for one of the attributes of interest. A correlation transformer can calculate various measures of association between the two input columns [92]. In this study, "corrcoef.m " is used to calculates a matrix "r" of correlation coefficients for input array, in which each row is an observation and each column is a variable.

If C is the covariance matrix, C = cov([x y]), then corrcoef([x y]) is the matrix whose (i,j)'th element is,

$$r(i,j) = C(i,j)/\sqrt{C(i,i) * C(j,j)} \tag{3.1}$$

The details of how to perform the correlation analysis of these data are given in Appendix C.

4. RESULTS

The breakdown of the identified stroke regions and their associated anatomical labels along with the volumes are presented in Table 4.1 and in Table 4.2 for two subject. Table 4.1 displays the results of a patient who has a lesion on the right side of his brain. Similarly, Table 4.2 displays a patient who has a lesion on his left side of brain. There are a couple of patients who have lesion on both left and right brains. Selecting the region of lesion in such a case is a two step procedure and is performed by first identifying the region on one side and then choosing the lesion on the other side.

Table 4.1
The label and volume of corresponding selected region in the Talairach atlas (Right selection)

Volume(mm^3)	Volume(%)	Region
6.60	37.6	Right Cerebrum.Sub-lobar.Thalamus.Gray Matter*
1.27	7.2	Right Cerebrum.Sub-lobar.Thalamus.Gray Matter.Medial Dorsal Nucleus
8.90	50.7	Right Cerebrum.Sub-lobar.Thalamus.Gray Matter.Ventral Lateral Nucleus
0.80	4.5	Right Cerebrum.Sub-lobar.Thalamus.Gray Matter.Ventral Anterior Nucleus
Total volume = 15.571 mm^3 (221 voxels) (0.43 x 0.43 x 0.43)		

Table 4.2
The label and volume of corresponding selected region in the Talairach atlas (Left selection)

Volume(mm^3)	Volume(%)	Region
3.82	0.9	Left Cerebrum.Sub-lobar.Extra-Nuclear.White Matter*
99.62	24.2	Left Cerebrum.Sub-lobar.Thalamus.Gray Matter.*
13.99	3.4	Left Cerebrum.Sub-lobar.Thalamus.Gray Matter.Ventral Posterior Lateral Nucleus
7.71	1.9	Left Cerebrum.Sub-lobar.Thalamus.Gray Matter.Mamillary Body
11.77	2.9	Left Cerebrum.Sub-lobar.Thalamus.Gray Matter.Medial Dorsal Nucleus
256.81	62.4	Left Cerebrum.Sub-lobar.Thalamus.Gray Matter.Ventral Lateral Nucleus
9.46	2.3	Left Cerebrum.Sub-lobar.Thalamus.Gray Matter.Venrtal Anterior Nucleus
8.11	2.0	Left Cerebrum.Sub-lobar.Thalamus.Gray Matter.Anterior Nucleus
Total volume = 411.2897 mm^3 (5173 voxels) (0.43 x 0.43 x 0.43)		

Table 4.3
Patient feature data

Number of patients (n)	43
Sex (n)	24 female, 19 male
The average age of patients (±SD; min-max)(year)	(±58.7.41 (15.20; 20-85))
Lateralization (n/%)	(20 left (%46.5); 21 right (%9); 2 bilateral (%4.5))
Follow-up period (the average month) (min-max)	(26.4 month±16.20) (3-64)
n: number, SD: standard deviation	

4.1 Anatomical findings

43 patients with thalamic infarct are classified by an expert neurologist into four groups as the anterior (anterior / anteromedial), the medial, lateral (inferolateral / posterolateral) and others (the posterior and central) [13]. The number of patients in each group, lateralization of the lesion, anatomic and clinical findings and neuropsychological findings are evaluated. General features of patients are presented in Table 4.3.

After all the regions for patients are selected by the expert neurologist, their absolute and percentage volume are computed using the developed graphical user interface. The stroke lesions are found to be localized to a maximum of 32 different regions with varying distributions for each subject. The mean distribution of these 32 regions over the patients is presented in Figure 4.3. Similarly, Figure 4.4 and Figure 4.5 show the same distribution for the male and female patients. When a t-test is performed, no statistical difference between female and male patients has been observed (p=0.5712).

Based on the expert neurologist's evaluation, among all the cerebral infarctions; 21 (49%) were left, 20 (46.5%) were right and 2 (4.5%) were two-sided one as can be seen in Figure 4.1. Among infarcts, 6 of them were anterior (4 left, 1 right, 1 bilateral), 11 of them were medial (5 left, 6 right), 17 of them were lateral (10 left, 7 right). With respect to 'others group', 4 posterior (1 left,3 right), 4 central(1 left, 3 right) were detected. This grouping is presented in Figure 4.2.

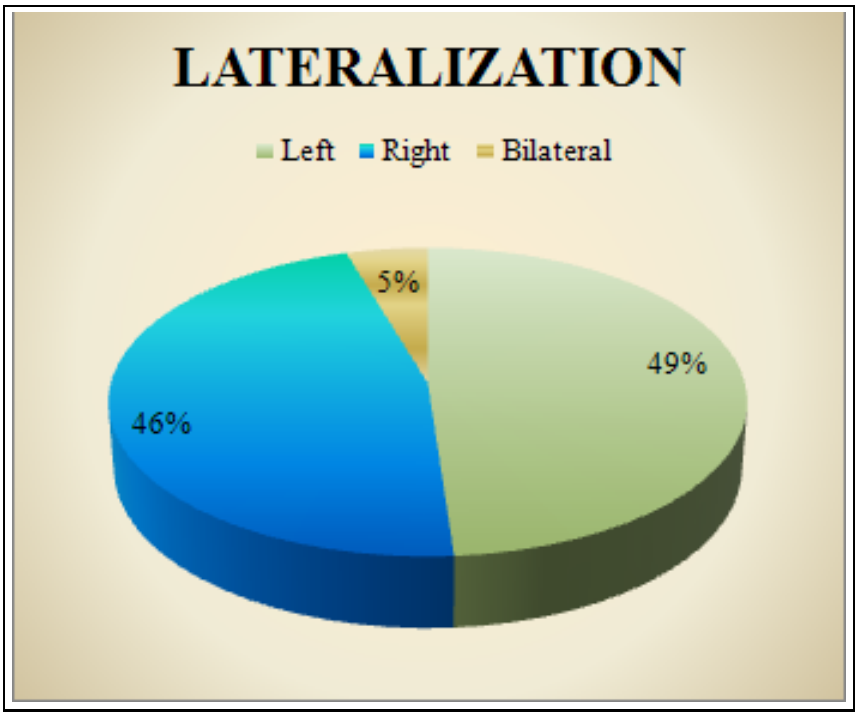

Figure 4.1 Lateralization of selected brain parts

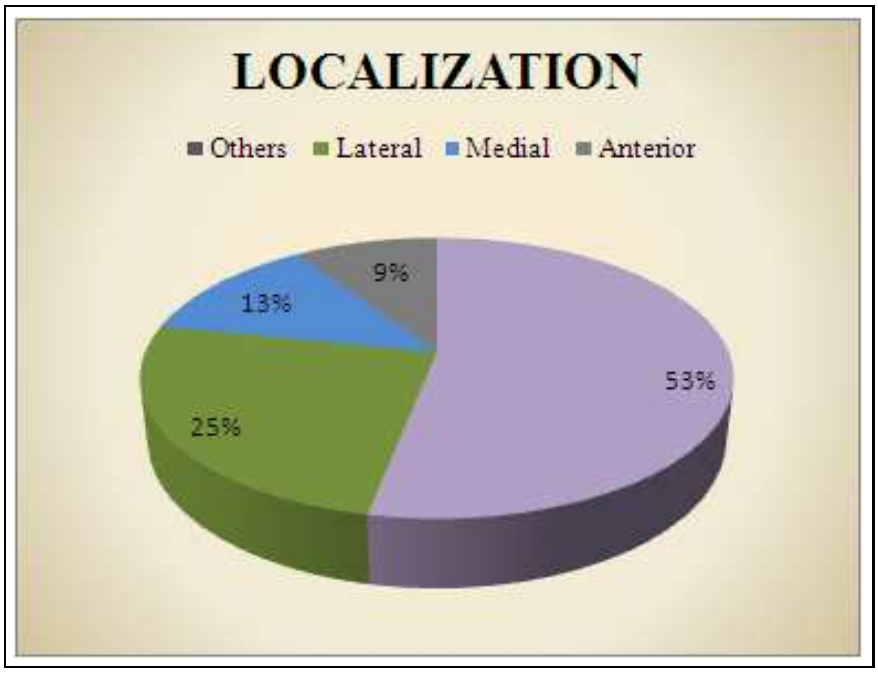

Figure 4.2 Localization of selected brain parts

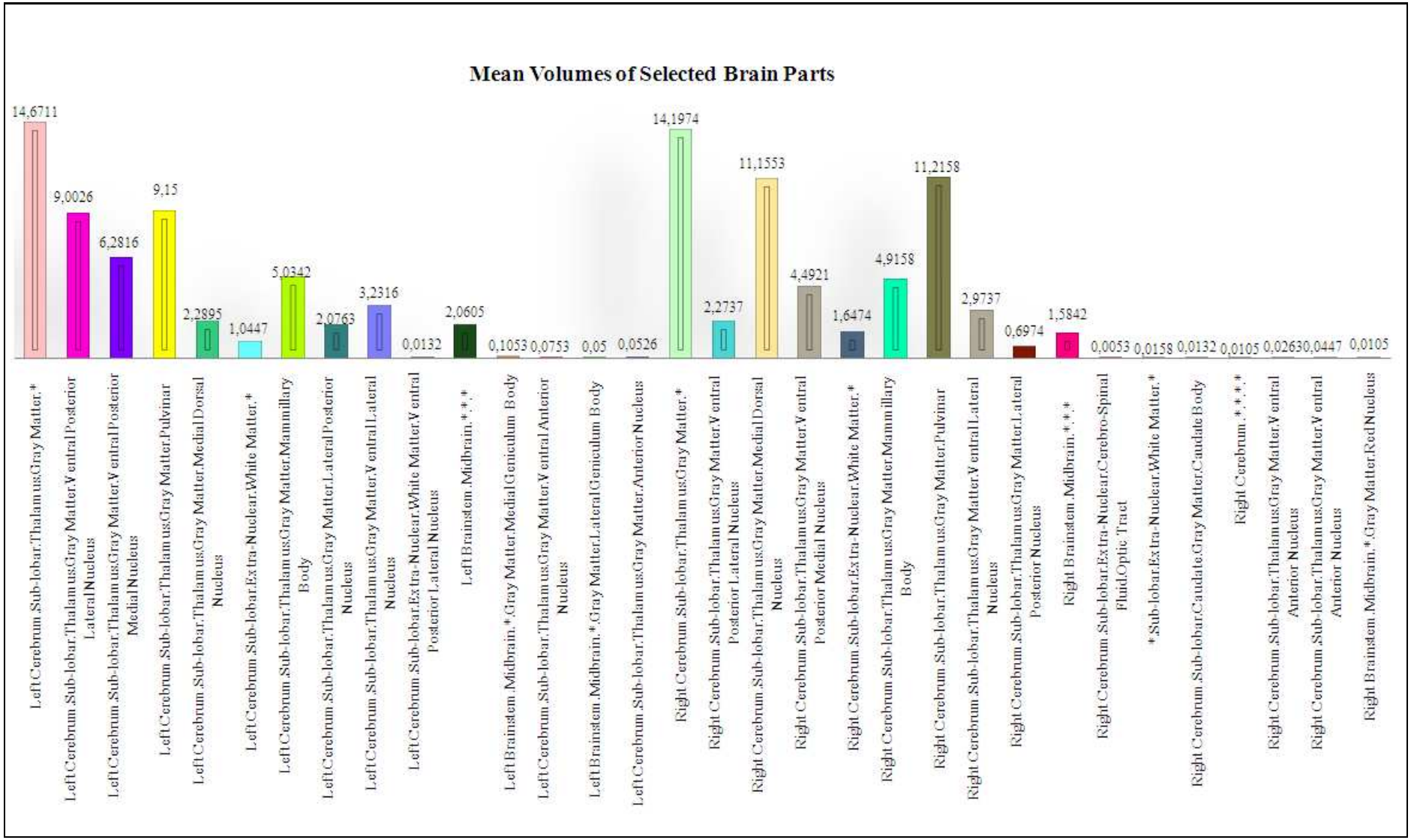

Figure 4.3 Mean volumes of selected brain parts

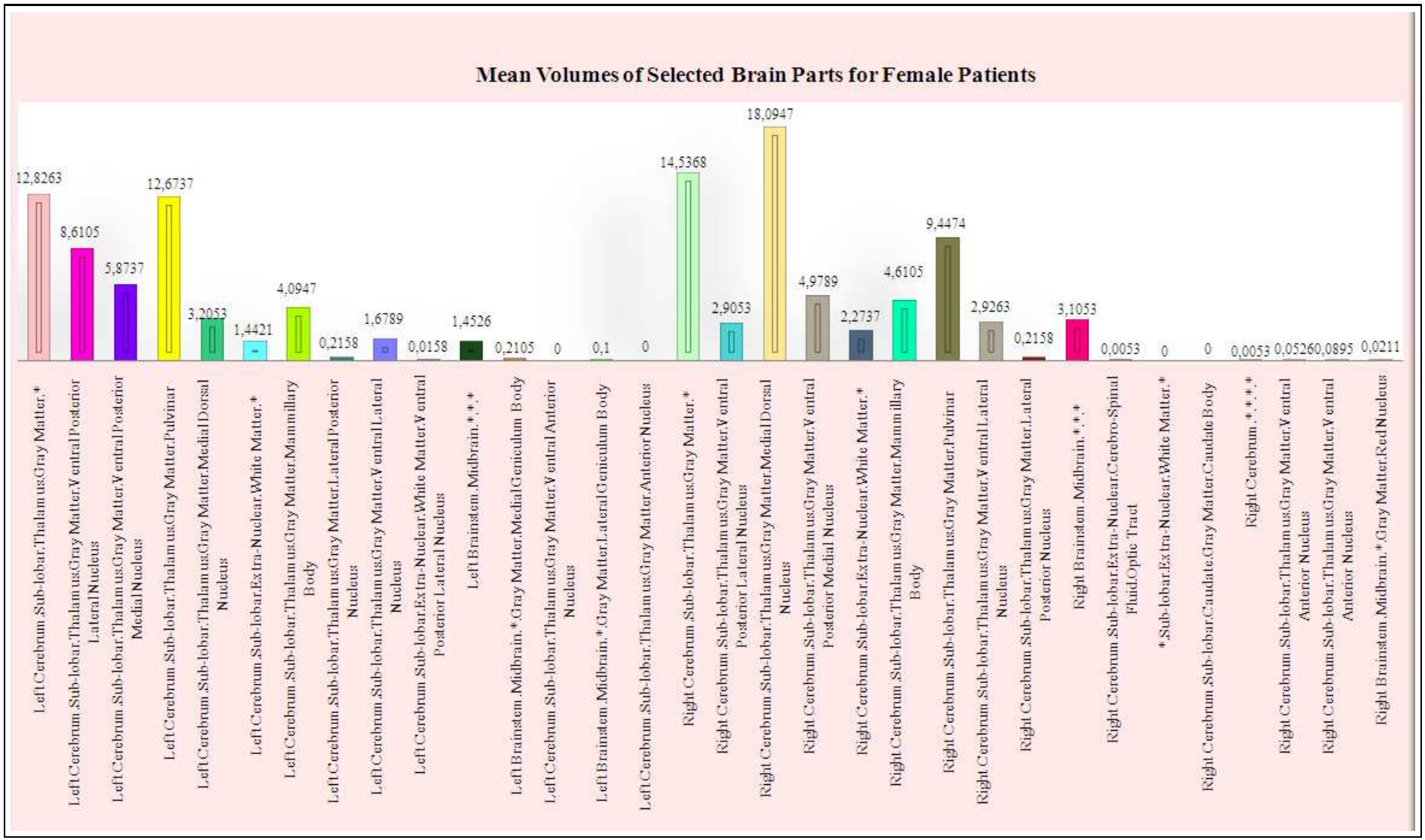

Figure 4.4 Mean volumes of selected brain parts for female patients

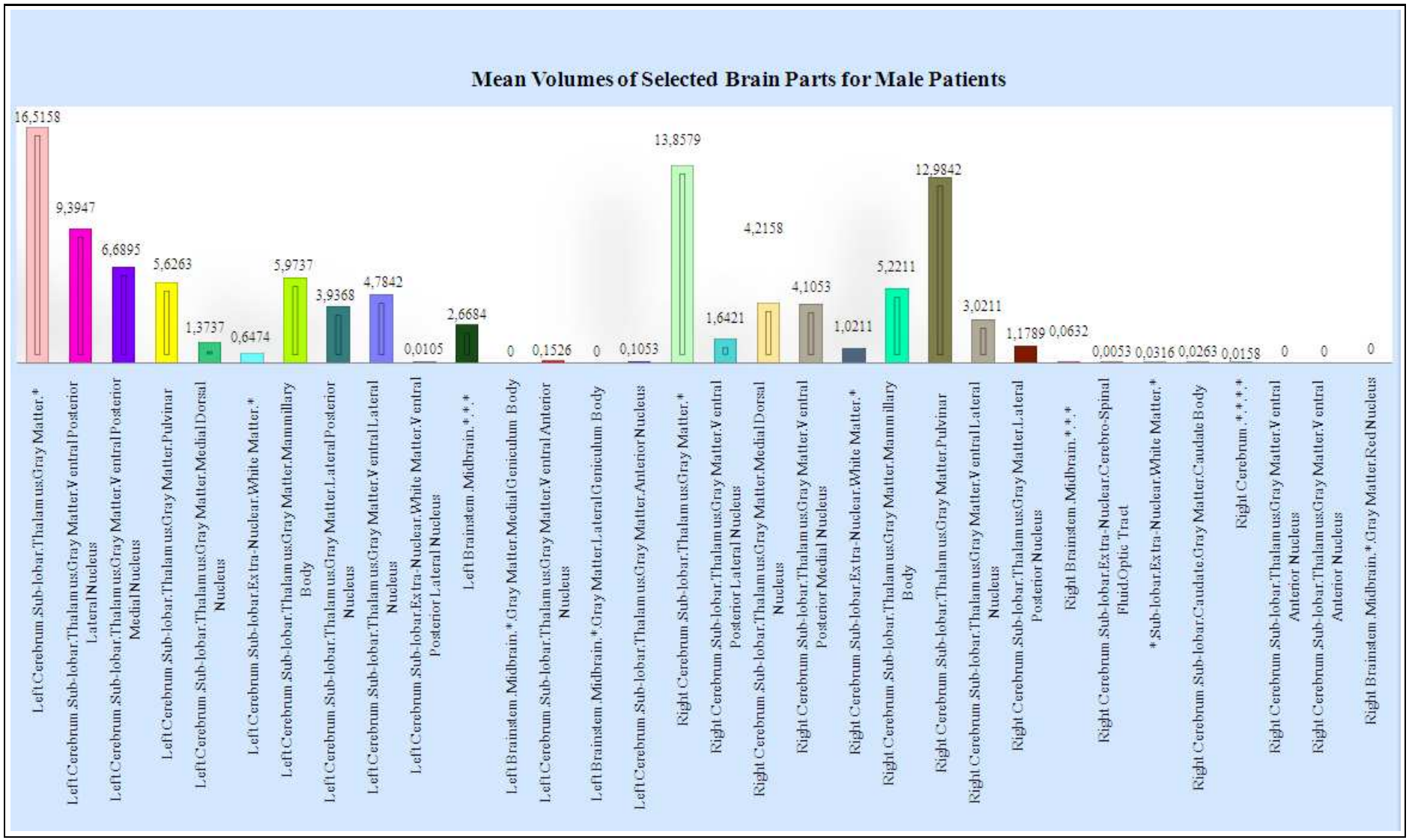

Figure 4.5 Mean volumes of selected brain parts for male patients

4.2 Correlation analysis of neuropsychologic tests (MMSE, FBI (-), FBI (disinhibition), BDI) and total volume of corresponding selected region in the Talairach atlas

Correlation analysis is performed to determine the extent to which the changes in the thalamic volume and distribution are related to the neuropsychological tests. In the Table 4.2, correlated regions are shown as bold. Although there is no significant correlation between MMSE and right lateral infarcts evaluation, a significant correlation is detected in patients with left and all the lateral thalamic infarction [13]. The regions labeled with 'Left Cerebrum.Sub-lobar. Thalamus.Gray Matter.*', 'Left Brainstem.Midbrain.*.*.*', 'Left Brainstem.Midbrain.*.Gray Matter.Medial Geniculum Body' are correlated with MMSE as can be seen in Table 4.5, ($p \leq 0.05$).

BDI, objectively assesses the degree of depression. There was no significant change with the evaluation of BDI for the patients with the right and left lateral thalamic infarct [13]. And also no correlation was found when correlated with BDI findings and total volume of corresponding selected region in the Talairach atlas. FBI is a scale to provide the criteria for the diagnosis of behavioral disorders within the patients demented with frontal lobe [77, 78]. We are provided with the evaluation scores of FBI(-) and FBI (disinhibition). The evaluation scores are significantly higher in both right and left thalamic infarction. This condition is regarded as another indication of deterioration the thalamus and the frontal lobe connections [13]. Furthermore, when FBI(-) and FBI (disinhibition) findings are correlated with total volume of corresponding selected region in the Talairach atlas. The correlations in the regions labeled with 'Left Cerebrum.Sub-lobar.Thalamus.Gray Matter.Lateral Posterior Nucleus' are statistically significant $p \leq 0.05$ as seen in Table 4.5. Therefore, these regions are considered to be correlated to FBI(-) and FBI (disinhibition).

Table 4.4
General features of patients who participated in neuropsychologic tests

Number of patients (n/ %)	17 / % 39.5
Sex (n)	8 female, 9 male
The average age of patients (±SD;min-max)(year)	(±64.41 (10.37; 41-84))
Lateralization (n/%)	10 Left(%58.8); 7 right(%41.2)
Follow-up period (the average month) (min-max)	(25.11±13.64) (3-55)
n: number, SD: standard deviation	

Table 4.5

Correlation analysis of neuropsychologic tests (MMSE, FBI(-), FBI (disinhibition), BDI) and total volume of corresponding selected region in the Talairach atlas

	MMSE	FBi(-)	FBi (disin)	BDI
Left Cerebrum.Sub-lobar. Thalamus.Gray Matter.*	**-0.53**	-0.0368	0.0436	0.0477
Left Cerebrum.Sub-lobar.Thalamus.Gray Matter.Ventral Posterior Lateral Nucleus	0.0117	0.4332	0.4212	0.2135
Left Cerebrum.Sub-lobar.Thalamus.Gray Matter.Ventral Posterior Medial Nucleus	-0.3113	0.069	0.0707	0.2494
Left Cerebrum.Sub-lobar.Thalamus.Gray Matter.Pulvinar	-0.2718	-0.02	0.2139	0.11933
Left Cerebrum.Sub-lobar.Thalamus.Gray Matter.Medial Dorsal Nucleus	*	*	*	*
Left Cerebrum.Sub-lobar.Extra-Nuclear.White Matter.*	-0.1039	-0.0525	0.0318	0.3482
Left Cerebrum.Sub-lobar.Thalamus.Gray Matter.Mammillary Body	-0.322	-0.1131	-0.0314	0.0311
Left Cerebrum.Sub-lobar.Thalamus.Gray Matter.Ventral Posterior Medial Nucleus	0.1732	-0.0187	-0.0332	-0.3359
Left Cerebrum.Sub-lobar.Thalamus.Gray Matter.Lateral Posterior Nucleus	0.1986	**0.7296**	**0.7535**	0.1093
Left Cerebrum.Sub-lobar.Extra-Nuclear.White Matter.Ventral Posterior Lateral Nucleus	0.2758	-0.1106	-0.178	0.2783
Left Brainstem.Midbrain.*.*.*	**-0.7452**	0.1678	0.0757	-0.1039
Left Brainstem.Midbrain.*.Gray Matter.Medial Geniculum Body	**-0.7548**	0.2996	0.1255	-0.1665
Left Cerebrum.Sub-lobar.Thalamus.Gray Matter.Ventral Anterior Nucleus	*	*	*	*
Left Brainstem.Midbrain.*.Gray Matter.Lateral Geniculum Body	-0.4626	-0.0773	-0.0214	0.0213
Left Cerebrum.Sub-lobar.Thalamus.Gray Matter.Anterior Nucleus	*	*	*	*
Right Cerebrum.Sub-lobar.Thalamus.Gray Matter.*	0.3033	-0.2726	-0.3543	-0.308
Right Cerebrum.Sub-lobar.Thalamus.Gray Matter.Ventral Posterior Lateral Nucleus	0.303	-0.144	-0.2726	-0.2322
Right Cerebrum.Sub-lobar.Thalamus.Gray Matter.Medial Dorsal Nucleus	0.0788	-0.1279	-0.2279	-0.1783

	MMSE	FBi(-)	FBi (disin)	BDI
Right Cerebrum.Sub-lobar.Thalamus.Gray Matter.Ventral Posterior Medial Nucleus	0.245	-0.1982	-0.2246	-0.1263
Right Cerebrum.Sub-lobar.Extra-Nuclear.White Matter.*	0.3868	-0.0211	-0.1072	-0.0715
Right Cerebrum.Sub-lobar.Thalamus.Gray Matter.Mammillary Body	0.1354	-0.1378	-0.2901	-0.2822
Right Cerebrum.Sub-lobar.Thalamus.Gray Matter.Pulvinar	0.2011	-0.2348	-0.1937	-0.1341
Right Cerebrum.Sub-lobar.Thalamus.Gray Matter.Ventral Lateral Nucleus	0.3806	-0.0226	-0.1151	-0.0701
Right Cerebrum.Sub-lobar.Thalamus.Gray Matter.Lateral Posterior Nucleus	0.3803	-0.0448	-0.1482	-0.0871
Right Brainstem.Midbrain.*.*.*	*	*	*	*
Right Cerebrum.Sub-lobar.Extra-Nuclear.Cerebro-Spinal Fluid.Optic Tract	*	*	*	*
.Sub-lobar.Extra-Nuclear.White Matter.	*	*	*	*
Right Cerebrum.Sub-lobar.Caudate.Gray Matter.Caudate Body	0.3868	-0.0211	-0.1072	-0.0715
Right Cerebrum.*.*.*.*	*	*	*	*
Right Cerebrum.Sub-lobar.Thalamus.Gray Matter.Ventral Anterior Nucleus x	*	*	*	*
Right Cerebrum.Sub-lobar.Thalamus.Gray Matter.Anterior Nucleus	*	*	*	*
Right Brainstem.Midbrain.*.Gray Matter.Red Nucleus	*	*	*	*

5. DISCUSSIONS

5.1 Expected contribution of using the GUI based Talairach atlas

A graphical user interface software for anatomical labelling and volumetric analysis of MR images of thalamic stroke patients is presented. The results are promising and suitable for choosing and labelling the desired region in the brain. The software may be useful not only for identifying thalamic stoke patients' region of lesion but also other patients with lesions in other regions. However, it is important to note that when it comes to locate a large lesion in the brain, a different type of normalization method may be necessary [40, 93, 94, 95].

Using a software with electronic atlases for picking lesions in the MR brain images can also make a contribution to neuroradiology and neurology, particularly given the increasing demand for the interpretation of brain scans. Introduction of new imaging modalities will also make the the interpretation scan more difficult. Therefore, new approaches for speeding up and simplifying the interpretation of brain scans, hence, decreasing the learning curve of neuroradiologists are required. In my opinion, the use of such software with electronic brain atlases may be a good solution. Neuroradiologists can potentially benefit from brain atlases by faster scan interpretation and communicate this information to other clinicians which may increase confidence, and speed up learning as discussed in Nowinski [96].

5.2 Incompleted anatomical regions (Regions lebelled with "*" sign in Table 4.1 and Table 4.2)

As can be seen in Table 4.1 and Table 4.2, there is a couple of regions labelled with "*' because of incompleted anatomical regions in the hierarchical level of the

atlas. It is useful to expand the search range to produce an extended list of label options. This approach resembles how authors utilize the Talairach atlas, to reassess nearby labels and pick the most probable candidate when such confusion arrises [30]. Labelling errors for coordinate-based methods can stem from incomplete anatomical matching by global spatial normalization in addition to the methodological differences [93]. Additionally, in order to control any labelling error, a neurologist may chose the lesion area manually on the Talairach Atlas and compare the results with our software results.

5.3 Comparison of registration and normalization with previous studies

There are many techniques in the scientific literature that show distinctive ways to make one brain match to the shape of another or to recognize corresponding points between two brains. Some of these have been implemented in an entirely automated way to label brain anatomy (gyrii or sulci) and fewer of these still have been evaluated beyond visual inspection, where image correspondence is mistaken for anatomic correspondence [97]. There exist methods that are readily presented for estimating and comparing the accuracy of nonlinear registration [98, 99, 100]. Future studies may focus on using these different types of nonlinear registration algorithms.

Fundamentally, the small deformation theory starts from the fact,that image correspondence can be achieved properly with a small degree of image transformation [40, 93]. We do not make use of any masking during spatial normalization in that lesions in our MR brain image are considerably small. However, it should be kept in mind that for spatial normalization of large brain lesions or deformations, methods like cost function masking are called for[40]. And however, more studies have to be done for normalization of large brain deformations, in particular, for stroke patients.

5.4 Future ideas for the correlation analysis results

It is obvious that neuropsychological tests have an important role for reviewing the range of mental processes from simple motor performance to complex reasoning and problem solving. Correlation analysis of neuropsychological tests (MMSE, FBI, BDI) with volume of selected regions in the Talairach atlas may help the interpretation of mental processes resulting the stroke region. Likewise, other neuropsychological tests may be used to determine the correlation of stroke region and neuropsychological test results.

6. CONCLUSIONS

Using Brain atlas in combination with software tools enables the exchange of volumetric data information quantifying stroke regions among clinicians and help the diagnosis and treatment of thalamic stroke patients more effectively and accurately.

For further investigation, new toolboxes [44, 60, 61], Webbased directories [34, 67, 69, 70, 30], new brain atlases, new imaging modalities and new registration and normalization methods may also be used.

Additionally, correlation analysis of neuropsychological tests (MMSE, FBI, BDI) with the volume of selected stroke regions in the Talairach atlas may relate the neuropsychological and neuroanatomical data to obtain a more objective diagnostic value.

APPENDIX A. REGISTRATION AND NORMALIZATION STEPS IN SPM5 SOFTWARE

SPM is a Matlab software package operating Statistical Parametric Mapping for neuroimaging data. In this study, SPM5 version is used and can be found at "http://www.fil.ion.ucl.ac.uk/spm/software/download.html". SPM is launched from within Matlab by typing spm at the Matlab prompt. (If the spm.m fuction is not found, make sure that whether the SPM package is added on your Matlabpath or not). SPM uses (only) Analyze format images. You'll need to convert the images from your scanner to this format. In Figure A.1, the SPM5 default-user software and in Figure A.2, the main help button are presented. More online help may be acquired via the main help button.

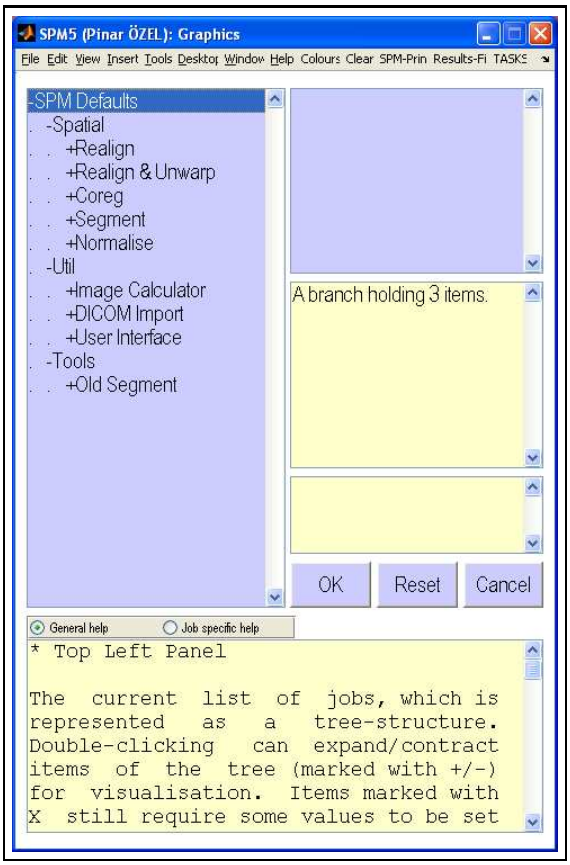

Figure A.1 The SPM5 default-user interface

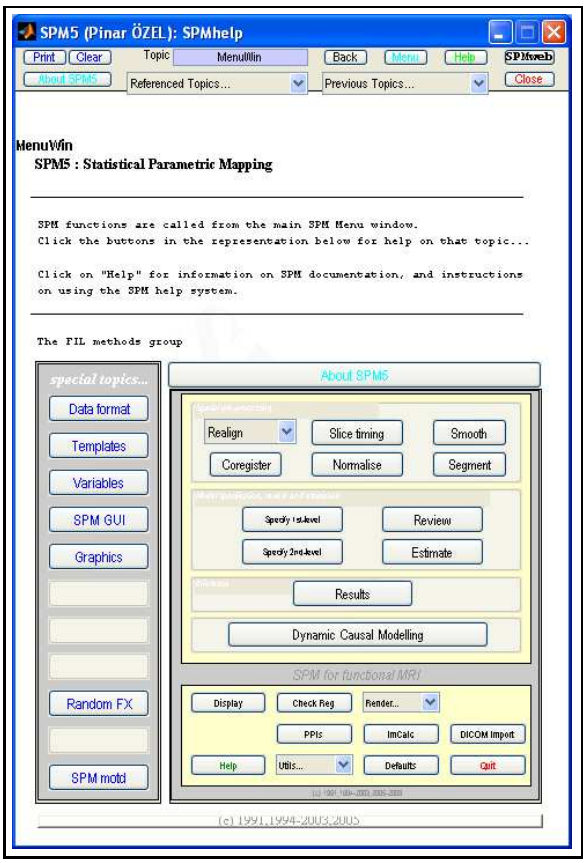

Figure A.2 The main help button

A.1 Registration step in SPM5

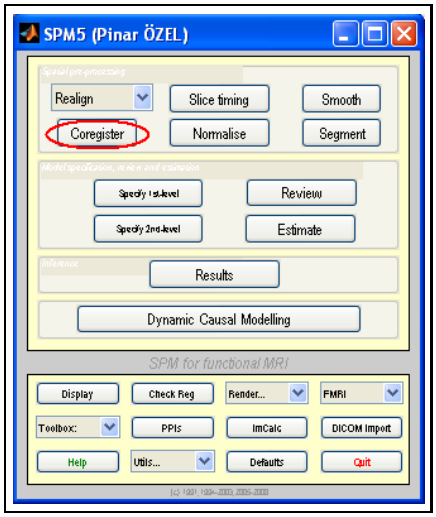

Figure A.3 Coregistration button in SPM5

Coregistration process starts with picking 'Coregister' button on SPM5 menu.

After this picking, you get the three options on the SPM5 user interface. Here, the necessary step for this study is to select "New.Coreg Estimate and Reslice" option because the relice is useful if two images have very different voxel sizes. In this study, the reference image and the source image have different voxel sizes.

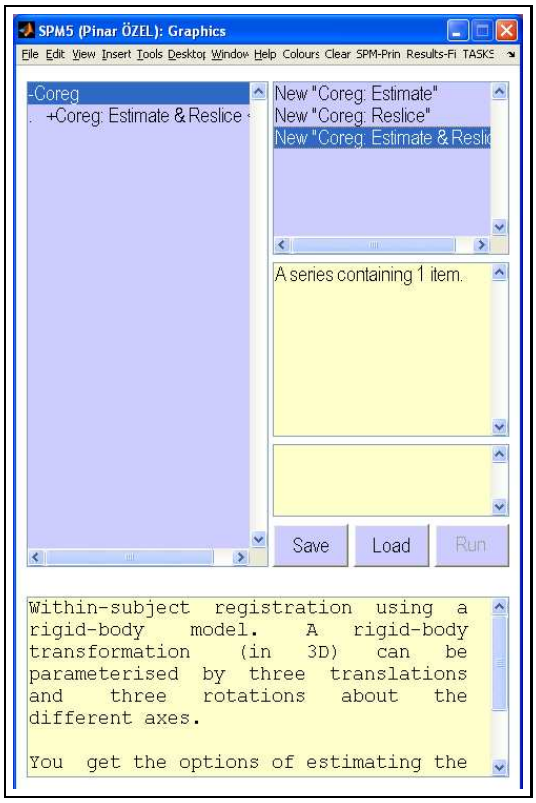

Figure A.4 Chosing coregistration type in SPM5

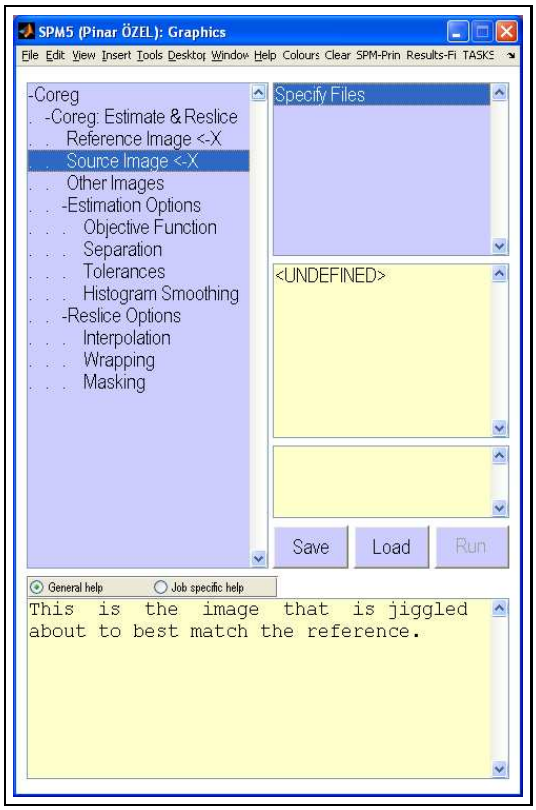

Figure A.5 Coreg:Estimate and Reslice Option

In Figure A.5, the reference image, source image and other image types, estimation and reslice options are shown. Other images are assumed as defaults used by SPM for estimating the match. Similarly, reslice options can be chosen from the menu for each of the three options however, in this study, this options are just defaults as well.

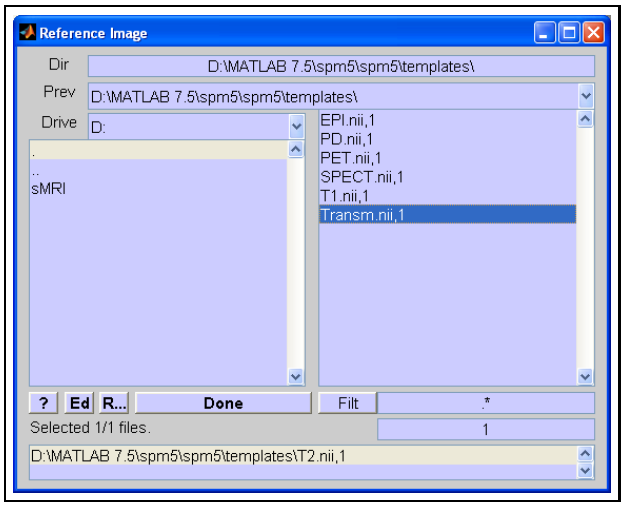

Figure A.6 The selection of reference image

As can be seen in Figure A.5, after picking the reference image button, T2.nii,1 image is selected among templates of SPM5 as reference image.

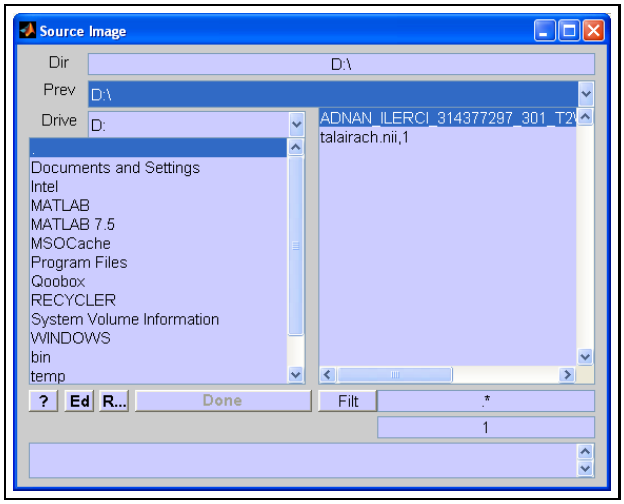

Figure A.7 The selection of source image

Source image that is 'jiggled about' to best match the reference and it is selected after picking source image button as in Figure A.5. Via using the file selector button, the *.img scan that the MRI data is obtained by user is selected.

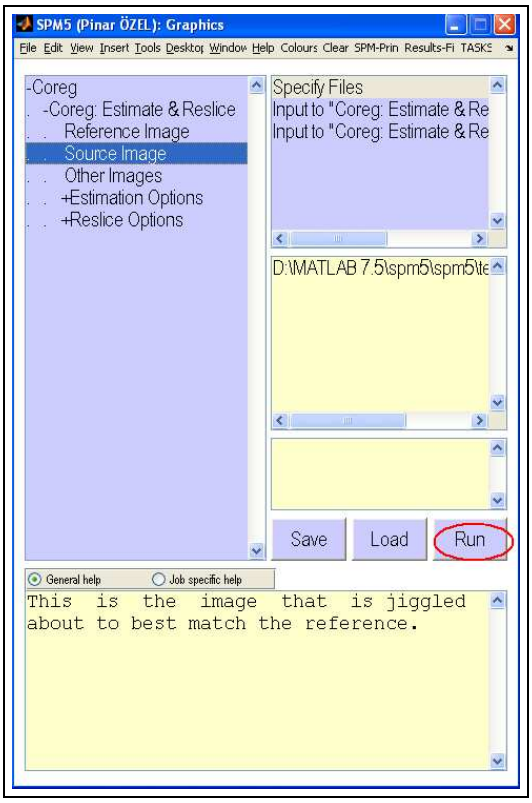

Figure A.8 Running process for coregistration

After all of these adjustments, the run button is picked. As a final part of coregistration, the voxel-to-voxel affine transformation matrix is shown, along with the histograms for the images in the original orientations, and the final orientations. The registered images are shown at the bottom. These images are also resliced to match the source image voxel-for-voxel. The resliced images are called the same as the originals except for they are prefixed by 'r' in the same subdirectory.

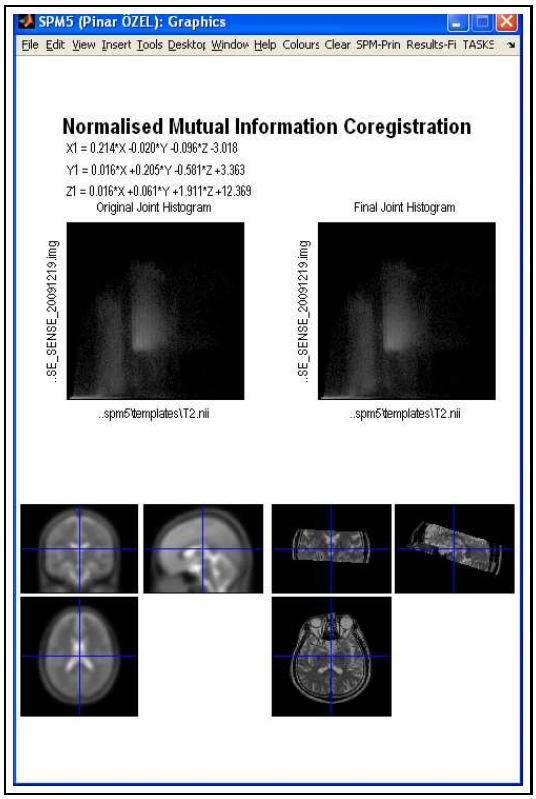

Figure A.9 The final part of coregistration

A.2 Normalization step in SPM5

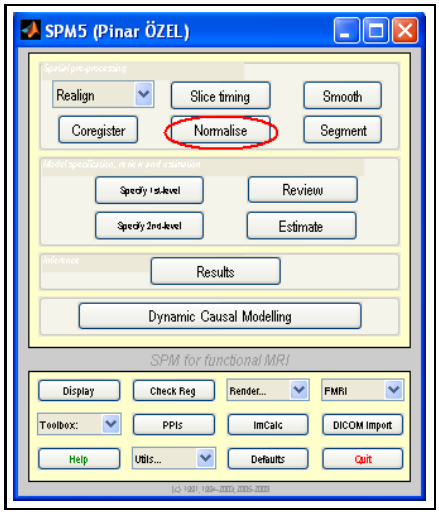

Figure A.10 Normalization button in SPM5

Normalization process starts with picking 'Normalise' button on SPM5 menu.

After this picking, one gets the three options on the SPM5 user interface. Here, the necessary step for this study is to select "New.Normalise: Estimate and Write" option. Estimate and Write will calculate what warps are needed to get from your selected image to the template, and will generate a file containing these images ending in "sn.mat" and then apply these warps to your selected image, producing a new image file with the same filename, but with an additional "w" at the front (standing for "warped").

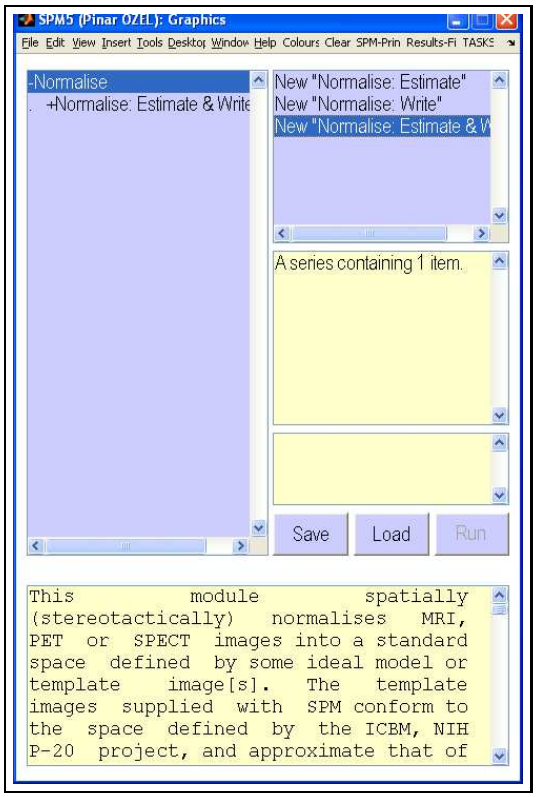

Figure A.11 Chosing normalization type in SPM5

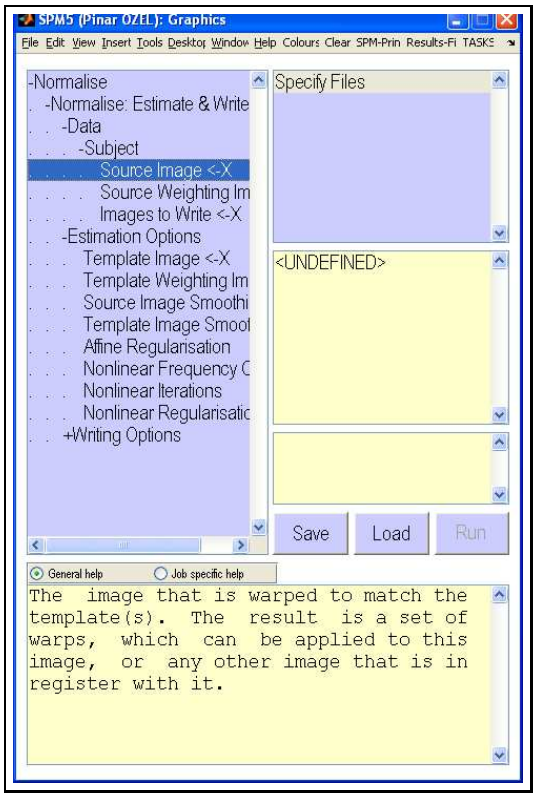

Figure A.12 Normalise: Estimate and Write option

In Figure A.11, the source image, the source weighting image, the image to write, estimation and write options are shown. Source weighting image are assumed as defaults used by SPM for estimating the match. Similarly, apart from template image in estimation options and voxel sizes in writing options, the other types of options are just defaults as well.

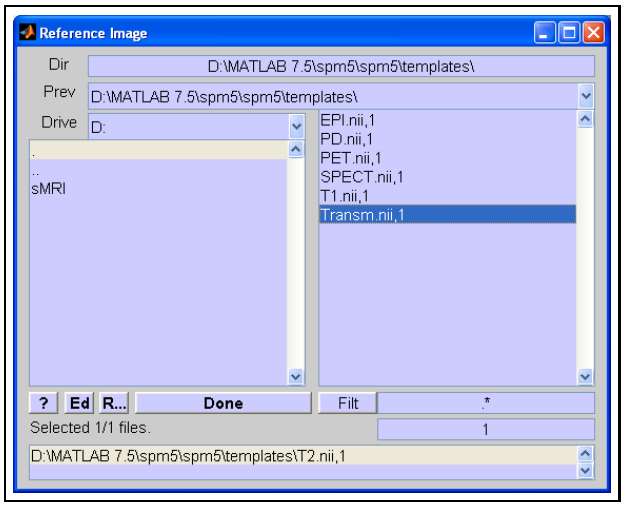

Figure A.13 The selection of template image

Similar to coregistration process, template image is the image that remains stationary. T2.nii,1 among the templates of SPM5 is selected in the file selector button for template image.

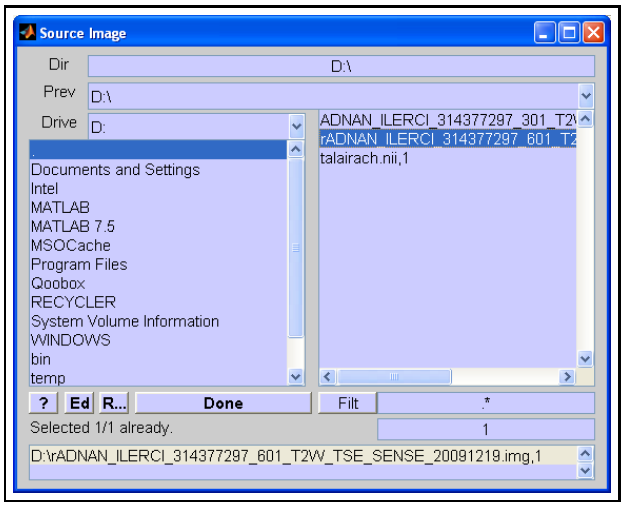

Figure A.14 The selection of source image

The image that is warped to match the template. Registered source image in coregistration process (r*.img) is used as source image in the study.

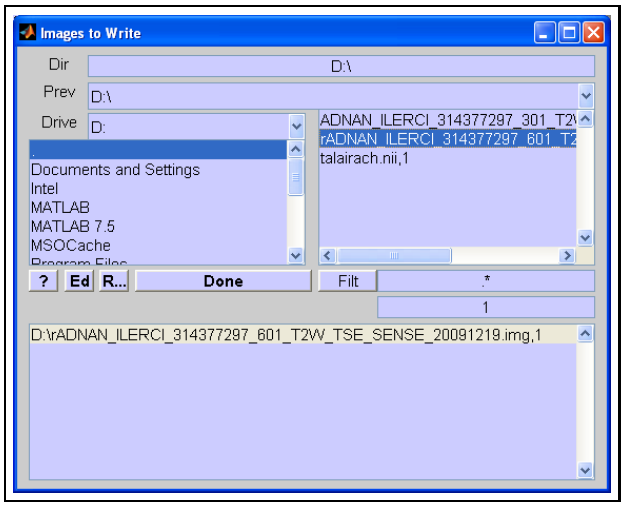

Figure A.15 The selection of "images to write "

It can be any images that are in register with the "source" image used to generate the param- eters. For this purpose, registered source image (r*.img) is selected in this process.

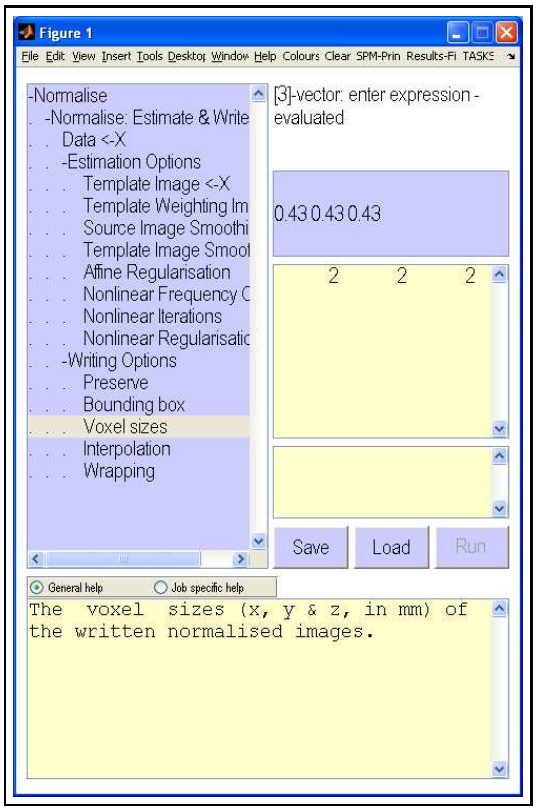

Figure A.16 Chosing voxel size

In order to increase the resolution of MR images, voxel sizes can be decreased. In the study, voxel size to warped out images is adjusted to 0.43*0.43*0.43 mm in the place of 2*2*2 mm.

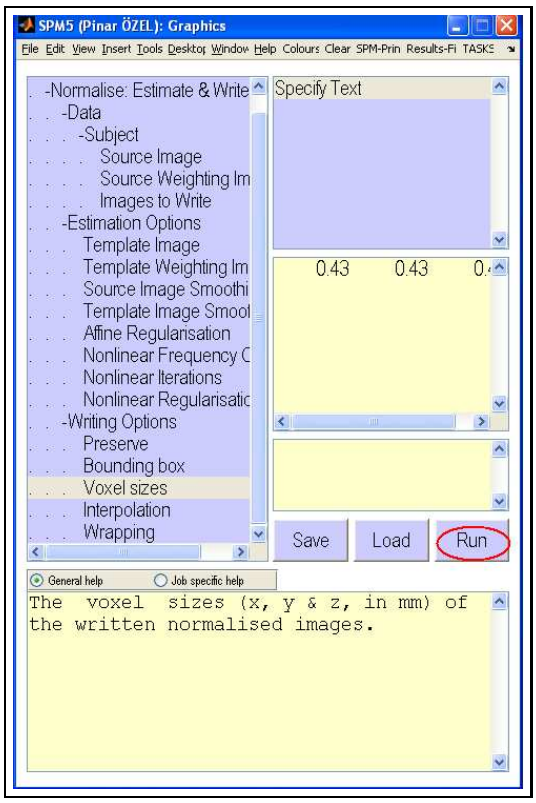

Figure A.17 Running process for normalization

After all of these adjustments, the run button is picked. All normalised *.img scans are written to the same subdirectory as the original *.img, prefixed with a 'w' (i.e. w*.img). The details of the transformations are displayed in the results window, and the parameters are saved in the "* sn.mat" file.

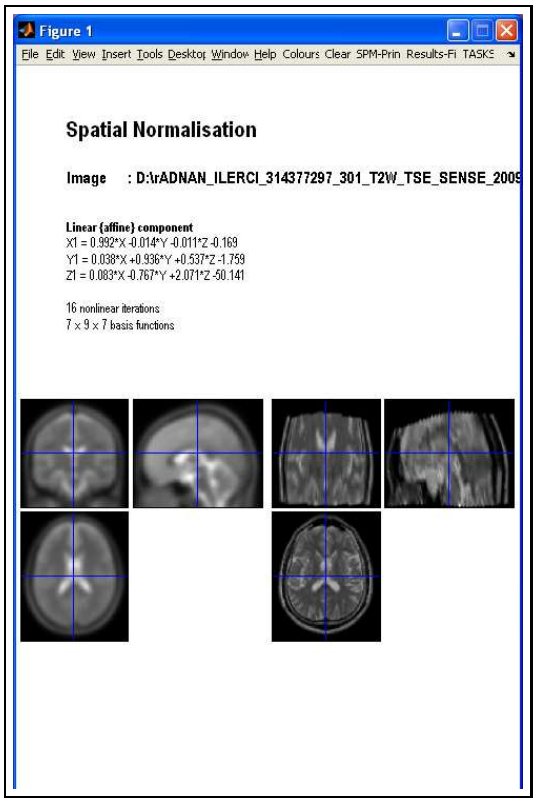

Figure A.18 The final part of normalization

As a result of registration and normalization process, addition to *.img file, r*.img file, w*.img file and sn.mat file are seen in the same subdirectory. When it comes to this point, in order to obtain a vector of structures containing image volume information, the normalized w*.img file is read via $VS = spm\_vol(D:\backslash w*.img)$ command. And in order to be read in entire image volumes $[VS1] = spm\_read\_vols(VS)$ command is used. A similar step is done for Talairah.nii file which can be separated as Talairah.img and Talairah.hdr by using related programmes.

Hereby, one must have four data at hand which are,

- A vector of structures containing image volume information
- XYZ matrix for entire image volumes
- A vector of structures containing Talairah image volume information

- XYZ matrix for entire Talairach image volumes

In the find_position.m file, these data are given VS, VS1, V1, V11 respectively. Addition to this, the range of Talairach labels and the knowledge of Talairach labels are necessary for implementing the GUI. And, in the find_position.m file, these are given “data”, “textdata” respectively.

For each subject, all of these data are included in a *.mat file. And if one demand to load a patient’s image, the mat file which belongs to this patient must be loaded in the GUI when picking “Load” button.

APPENDIX B. MATLAB scripts for GUI

B.1 tal_gui.m

```
function varargout = tal_gui(varargin)

% TAL_GUI Mfile for tal_gui.fig
% TAL_GUI, by itself, creates a new TAL_GUI or raises the existing singleton*.
%H = TAL_GUI returns the handle to a new TAL_GUI or the handle to the existing singleton*.
%TAL_GUI('CALLBACK', hObject, eventData, handles,...) calls the local function named CALLBACK in TAL_GUI.M with the given input arguments
%TAL_GUI ('Property','Value',...) creates a new TAL_GUI or raises the existing singleton*. Starting from the left, property value pairs are applied to the GUI before tal_gui_OpeningFunction gets called.
% An unrecognized property name or invalid value makes property application stop. All inputs are passed to tal_gui_OpeningFcn via varargin.
% *See GUI Options on GUIDE's Tools menu. Choose "GUI allows only one instance to run (singleton)".
% See also: GUIDE, GUIDATA, GUIHANDLES

gui_Singleton = 1;

gui_State = struct('gui_Name', mfilename, 'gui_Singleton',...
gui_Singleton, 'gui_OpeningFcn',@tal_gui_OpeningFcn,..
'gui_OutputFcn', @tal_gui_OutputFcn, 'gui_LayoutFcn', [ ] ,'gui_Callback', [ ]);

if nargin && ischar(varargin1)

gui_State.gui_Callback = str2func(varargin1);

end

if nargout

[varargout1:nargout] = gui_mainfcn(gui_State, varargin:);

else

gui_mainfcn(gui_State, varargin:);
```

```
end

% End initialization code - DO NOT EDIT
 %— Executes just before tal_ gui is made visible.

function tal_gui_OpeningFcn(hObject, eventdata, handles, varargin)

% This function has no output args, see OutputFcn. hObject handle to figure
% reserved - to be defined in a future version of MATLAB handles structure with
handles and user data (see
% )varargin command line arguments to tal_ gui (see VARARGIN)
% Choose default command line output for tal_ gui

handles.output = hObject;

% Update handles structure

guidata(hObject, handles);

% UIWAIT makes tal_gui wait for user response (see UIRESUME uiwait(handles.figure1);
% — Outputs from this function are returned to the command line.
function varargout = tal_gui_OutputFcn(hObject, eventdata, handles)

% varargout cell array for returning output args (see VARARGOUT);
% hObject handle to figure reserved - to be defined in a future version of MATLAB
handles structure with handles
%and user data (see GUIDATA)
%Get default command line output from handles structure
varargout1 = handles.output;

% — Executes on button press in pushbutton1.

function pushbutton1_Callback(hObject, eventdata, handles)

% hObject handle to pushbutton1 (see GCBO)
% eventdata reserved - to be defined in a future version of MATLAB
% handles structure with handles and user data (see GUIDATA)
%struct -> Vs
% -> Vs1
axis off;
%h=figure('position',[50 50 ii*1.5 jj*1.5]);

i=handles.i;
```

```
m1=squeeze(handles.Vs1(:,:,i));

axes(handles.axes1);

imagesc(m1,[handles.cmin handles.cmax]);colormap gray;axis ij;

axes(handles.axes2);

cla;

if length(find(handles.I2(:,:,i)>0))>0

axes(handles.axes2);

imagesc(m1,[handles.cmin handles.cmax]);colormap gray;hold on;axis ij;

[Px,Py]=find( handles.I2(:,:,handles.i)>0);

plot(Px,Py,'r');

end

axes(handles.axes1);

if length(find(handles.I2(:,:,i)>0))>0

axes(handles.axes1);

imagesc(m1,[handles.cmin handles.cmax]);colormap gray;hold on;axis ij;

[Px,Py]=find( handles.I2(:,:,handles.i)>0);

plot(Px,Py,'r');

end
%I2=roipoly;

%[Ix,Iy]=find(I2>0);co=[Iy Ix];
% — Executes during object creation, after setting all properties.

function figure1_CreateFcn(hObject, eventdata, handles)

% hObject handle to figure1 (see GCBO)
% eventdata reserved - to be defined in a future version of MATLAB
%handles empty - handles not created until after all CreateFcns called

i=1;

handles.i=i;
```

```
%handles.V1=evalin('base','V1');

Vs1=evalin('base','Vs1');

[cmin]=min(Vs1(:));[cmax]=max(Vs1(:));

handles.Vs1=Vs1;

handles.cmin=cmin;

handles.cmax=cmax;

[ii,jj,kk]=size(Vs1);

handles.ii=ii;handles.jj=jj;handles.kk=kk;

handles.I2=zeros(jj,ii,kk);

handles.Vmat=evalin('base','Vs.mat');

handles.V1=evalin('base','V1');

handles.V11=evalin('base','V11');

handles.Vs=evalin('base','Vs');

handles.textdata=evalin('base','textdata');

handles.data=evalin('base','data');

%handles.Vtalmat=evalin('base','V1.mat');

guidata(hObject,handles);

% — Executes on button press in pushbutton2.

function pushbutton2_Callback(hObject, eventdata, handles)

% hObject handle to pushbutton2 (see GCBO)
% eventdata reserved - to be defined in a future version of MATLAB
% handles structure with handles and user data (see GUIDATA)

if handles.i==handles.kk

else

handles.i=handles.i+1;

end
```

```
set(handles.edit1,'String',[num2str(handles.i) ' / ' num2str(handles.kk) ]);

guidata(hObject,handles);

pushbutton1_Callback(hObject, eventdata, handles);

% — Executes on button press in pushbutton3.

function pushbutton3_Callback(hObject, eventdata, handles)

% hObject handle to pushbutton3 (see GCBO)
% eventdata reserved - to be defined in a future version of MATLAB
% handles structure with handles and user data (see GUIDATA)


if handles.i==1

else

handles.i=handles.i-1;

end

set(handles.edit1,'String',[num2str(handles.i) ' / ' num2str(handles.kk) ]);

guidata(hObject,handles);

pushbutton1_Callback(hObject, eventdata, handles);

% — Executes on button press in pushbutton4.

function pushbutton4_Callback(hObject, eventdata, handles)

% hObject handle to pushbutton4 (see GCBO)
% eventdata reserved - to be defined in a future version of MATLAB
% handles structure with handles and user data (see GUIDATA)


T=handles.Vs1(:,:,handles.i);

cmin=min(T(:));

cmax=max(T(:));

set(gca,'clim',[cmin cmax]);

% — Executes on button press in pushbutton5.

function pushbutton5_Callback(hObject, eventdata, handles)
```

```
% hObject handle to pushbutton5 (see GCBO)
% eventdata reserved - to be defined in a future version of MATLAB
% handles structure with handles and user data (see GUIDATA)

set(gca,'clim',[handles.cmin handles.cmax]);

% — Executes on button press in pushbutton6.

function pushbutton6_Callback(hObject, eventdata, handles)

% hObject handle to pushbutton6 (see GCBO)
% eventdata reserved - to be defined in a future version of MATLAB
% handles structure with handles and user data (see GUIDATA)

handles.I2(:,:,handles.i)=handles.I2(:,:,handles.i)*0;

I2=roipoly;

handles.I2(:,:,handles.i)=I2';

guidata(hObject,handles);

pushbutton1_Callback(hObject, eventdata, handles);

function edit1_Callback(hObject, eventdata, handles)

% hObject handle to edit1 (see GCBO)
% eventdata reserved - to be defined in a future version of MATLAB
% handles structure with handles and user data (see GUIDATA)
% Hints: get(hObject,'String') returns contents of edit1 as text
% str2double(get(hObject,'String')) returns contents of edit1 as a double
% — Executes during object creation, after setting all properties.

function edit1_CreateFcn(hObject, eventdata, handles)

% eventdata reserved - to be defined in a future version of MATLAB
% handles empty - handles not created until after all CreateFcns called
% Hint: edit controls usually have a white background on Windows.
% See ISPC and COMPUTER.

if ispc && isequal(get(hObject,'BackgroundColor'),...
get(0,'defaultUicontrolBackgroundColor'))

set(hObject,'BackgroundColor','white');

end
```

```
% — Executes on button press in pushbutton7.

function pushbutton7_Callback(hObject, eventdata, handles)

% hObject handle to pushbutton7 (see GCBO)
% eventdata reserved - to be defined in a future version of MATLAB
% handles structure with handles and user data (see GUIDATA)

c=[ ];

for k=1:handles.kk

K=squeeze(handles.I2(:,:,k));

[I]=find(K>0);

if length(I)>0

[Ix,Iy]=ind2sub([handles.ii handles.jj],I);

c=[c;Ix Iy ones(length(Ix),1)*k];

end

end

Pix=c;

I2=handles.I2;

save Pix.mat I2;

[posname]=find_pos(handles.Vs,handles.Vs1,handles.data,...
handles.textdata,handles.V1,handles.V11);

save Pix.mat I2 posname

%D1=handles.Vmat*[c ones(length(c),1)]';D1=D1(1:3,:)';
%D2=icbm_spm2tal(D1);
%Pix=D2;
%Pix=inv(handles.Vtalmat)*[D2 ones(length(D2),1)]';Pix=Pix(1:3,:)';
```

B.2 find_position.m

```
function [posname]=find_pos(Vs,Vs1,data,textdata,V1,V11)

load Pix

[ii,jj,kk]=size(Vs1);

[A1,A2,A3]=ind2sub([jj ii kk],find(I2>0));

for i=1:length(A1)

pp=Vs.mat*[A2(i) A1(i) A3(i) 1]';pp=pp(1:3);

pp1=icbm_spm2tal(pp);

pp2=inv(V1.mat)*[pp1' 1]';pp2=fix(pp2(1:3));

d(i)=V11(pp2(1),pp2(2),pp2(3))+1;

end

a=hist(d,[1:1106]);

b=find(a>0);

T=0;

posname=struct();

for j=1:length(b)

posname(j).name= textdata(b(j),2);

x=diag(Vs.mat);x=abs(x(1)*x(2)*x(3));

posname(j).size= a(b(j))*x;

T=T+posname(j).size;

end

x=diag(Vs.mat);

f=fopen('result.txt','wt');

fprintf(f,['TotalVolume =' num2str(T)'mm^3('num2str(sum(a(b)))'voxels)...
('num2str(abs(x(1)))'x'num2str(abs(x(2)))'x')
```

$num2str(abs(x(3)))') \setminus n \setminus n']);$

$fprintf(f,'\nVolume\,in\,mm^3 \setminus t \setminus t\%\%Volume \setminus t \setminus tRegion \setminus n');$

$fprintf(f,'----------\n');$

$for j = 1 : length(b)$

$fprintf(f,'\%5.2f \t\t\%2.1f \t\t\%s\n', posname(j).size, 100*posname(j).size/(T), ...$
$cell2mat(posname(j).name));$
$fprintf(f,'\n');$

end

$fclose(f);$

APPENDIX C. The implementation of the correlation analysis

Table C.1
The results of neuropsychological tests

The range of patients	MMSE	FBi(-)	FBi disin	BDI
1	24	6	5	32
2	23	3	3	10
3	26	0	0	11
4	28	19	13	14
5	27	2	6	4
6	27	3	3	10
7	27	4	3	0
8	27	15	6	23
9	29	0	0	3
10	22	11	5	3
11	27	5	2	5
12	30	4	2	7
13	28	2	3	13
14	26	4	2	10
15	28	1	1	3
16	29	1	1	0
17	28	5	3	24

“ corrcoef.m” file is operated as $[r, p] = corrcoef = ([xy])$, where x and y are columns vectors. Addition to “r” coefficient value, $[r, p] = corrcoef([xy])$ also returns p, a matrix of p-values for testing the hypothesis of no correlation. Each p-value is the probability of getting a correlation as large as the observed value by random

chance, when the true correlation is zero. If p(i,j) is small, say less than 0.05, then the correlation r(i,j) is significant.

In present study, "x" value is assumed as one of the selected stroke region for each subject. "y" value is assumed as one of the results for neuropsychological tests mentioned in chapter 1.

In order to show "the range of patients for neuropysiological tests", "the range of patients during calculating the mean distributions" and "the selected stroke region for each subject", Table C.3, Table C.4, Table C.5, Table C.6 are given.[1] In fact, Table C.3, Table C.4, Table C.5, Table C.6 are a part of Table C.2 which is already a simulation table for the distribution of selected stroke regions. In order to be visualized, TableC.2 is presented.

As can be realized in Table C.3, Table C.4, Table C.5, Table C.6, a group of patient's values are evaluated for the correlation analysis . This group is the lateral group of thalamic infarction in Figure 4.4. According to this, the patients for neuropysiological tests are numbered in Table C.1 (It can been when being looked at the first column) and the same numbers are used in Table C.3, Table C.4, Table C.5, Table C.6 (similarly look at first column at these Tables). These number are bold at these tables. For each correlation analysis test, one column is taken in Table C.1 and one column is taken in Table C.3, Table C.4, Table C.5, Table C.6 with the same range at first column compared to Table C.1.

When these column vectors are correlated via $[r, p] = corrcoef([xy])$command, two results return as "r" and "p". Then, among the correlation values, those which have " $p \leq 0.05$" are taken for evaluations significantly. In Table 4.5, the results are presented.

The mean distribuiton values can also be acquired when the columns are added

[1]In Table C.3, Table C.4, Table C.5, Table C.6, a couple of the selected stroke regions whose values has already empty are eliminated in order the tables to be squeezed in a page

up on their own. Additionally, in Table C.3, Table C.4, Table C.5, Table C.6, the italic values show the female patients. Separately, the mean distribuiton for female and male groups can be acquired when the columns are added up on their own (Figure 4.3, Figure 4.4 and Figure 4.5).

Table C.2
The simulation table for the distribution of selected stroke regions

A1	A2
B1	B2

Table C.3
The distribution of selected stroke region for each subject (A1 Part)

The range of patients for the neuropsychologic tests	The range of patients during calculating the mean distributions	Left Cerebrum.Sub-lobar. Thalamus.Gray Matter.*	Left Cerebrum.Sub-lobar.Thalamus.Gray Matter.Ventral Posterior Lateral Nucleus	Left Cerebrum.Sub-lobar.Thalamus.Gray Matter.Ventral Posterior Medial Nucleus	Left Cerebrum.Sub-lobar.Thalamus.Gray Matter.Pulvinar	Left Cerebrum.Sub-lobar.Thalamus.Gray Matter.Medial Dorsal Nucleus	Left Cerebrum.Sub-lobar.Extra-Nuclear.White Matter.*	Left Cerebrum.Sub-lobar.Thalamus.Gray Matter.Mammillary Body	Left Cerebrum.Sub-lobar.Thalamus.Gray Matter.Ventral Posterior Medial Nucleus	Left Cerebrum.Sub-lobar.Thalamus.Gray Matter.Lateral Posterior Nucleus	Left Cerebrum.Sub-lobar.Extra-Nuclear.White Matter.Ventral Posterior Lateral Nucleus	Left Brainstem.Midbrain.*.*.*	Left Brainstem.Midbrain.*.Gray Matter.Medial Geniculum Body	Left Brainstem.Midbrain.*.Gray Matter.Lateral Geniculum Body
1	1	***15.7***	***1.1***	***34.5***	***48.8***									
	2													
	3	41.6				0.7	0.3	20.4				37		
	4	*26.8*	*7.7*	*8.2*	*2.2*	*19.4*		*6.2*	*4.1*	*25.4*				
12	5													
13	*6*													
14	*7*													
4	8	**6.1**	**83.9**	**6.7**			**1.5**		**0.9**	**1**				
	9	*42.8*			*100*	*41.5*		*9.2*		*6.5*				
2	*10*	***16.1***	***48.9***	***14.9***			***9.4***	***0.1***				***7.3***	***1.4***	***1.9***
3	11	***49.3***	***35.5***	***4.5***	***8.1***		***2.7***							
	12	69.8	0.9			3.7			3	22.5				
	13													
5	14	**31**	**9.3**	**5.2**	**49.6**		**4.8**							
	15													
	16	55.5				13.7		28.4		2.4				
15	17													
6	18	**13**	**14.6**	**68.4**	**3.6**			**0.1**		**0.3**				
16	19													

Table C.4
The distribution of selected stroke region for each subject(A2 Part)

The range of patients for the neuropsychologic tests	The range of patients during calculating the mean distributions	Right Cerebrum.Sub-lobar.Thalamus.Gray Matter.*	Right Cerebrum.Sub-lobar.Thalamus.Gray Matter.Ventral Posterior Lateral Nucleus	Right Cerebrum.Sub-lobar.Thalamus.Gray Matter.Medial Dorsal Nucleus	Right Cerebrum.Sub-lobar.Thalamus.Gray Matter.Ventral Posterior Medial Nucleus	Right Cerebrum.Sub-lobar.Thalamus.Gray Matter.Mammillary Body	Right Cerebrum.Sub-lobar.Thalamus.Gray Matter.Mammillary Body	Right Cerebrum.Sub-lobar.Thalamus.Gray Matter.Pulvinar	Right Cerebrum.Sub-lobar.Thalamus.Gray Matter.Ventral Lateral Nucleus	Right Cerebrum.Sub-lobar.Thalamus.Gray Matter.Lateral Posterior Nucleus	Right Brainstem.Midbrain.*.*.	Right Cerebrum.Sub-lobar.Extra-Nuclear.Cerebro-Spinal Fluid.Optic Tract	*.Sub-lobar.Extra-Nuclear.White Matter.*	Right Cerebrum.Sub-lobar.Caudate.Gray Matter.Caudate Body	Right Cerebrum.*.*.*.*
1	*1*														
	2	10.3				2.7		86.5					0.6		
	3														
	4														
12	5	**4.6**	**11.8**		**3.7**	**1.7**			**57.4**	**20.3**				**0.5**	
13	*6*	***21.5***			***52.9***			***25.5***							
14	*7*	***22.7***	***16.4***	***3.5***	***24.2***		***25.1***		***4.1***	***4.1***					
4	8														
	9	*27.1*	*35.1*		*5.4*	*21.7*			*10.6*						
2	*10*														
3	*11*														
	12														
	13	*4.3*		*1.3*				*94.3*							
5	14														
	15	*16.8*		*68.7*		*0.3*	*1.3*	*12.9*			*0.1*				
	16														
15	17	**32.4**		**0.1**	**6.1**		**8.9**	**50.4**		**2.1**					
6	18														
16	19	**29.2**	**15.5**	**2.4**	**30.2**		**22.8**								

Table C.5
The distribution of selected stroke region for each subject(B1 part)

The range of patients for the neuropsychologic tests	The range of patients during calculating the mean distributions	Left Cerebrum.Sub-lobar. Thalamus.Gray Matter.*	Left Cerebrum.Sub-lobar.Thalamus.Gray Matter.Ventral Posterior Lateral Nucleus	Left Cerebrum.Sub-lobar.Thalamus.Gray Matter.Ventral Posterior Medial Nucleus	Left Cerebrum.Sub-lobar.Thalamus.Gray Matter.Pulvinar	Left Cerebrum.Sub-lobar.Thalamus.Gray Matter.Medial Dorsal Nucleus	Left Cerebrum.Sub-lobar.Extra-Nuclear.White Matter.*	Left Cerebrum.Sub-lobar.Thalamus.Gray Matter.Mammillary Body	Left Cerebrum.Sub-lobar.Thalamus.Gray Matter.Ventral Posterior Medial Nucleus	Left Cerebrum.Sub-lobar.Thalamus.Gray Matter.Lateral Posterior Nucleus	Left Cerebrum.Sub-lobar.Extra-Nuclear.White Matter.Ventral Posterior Lateral Nucleus	Left Brainstem.Midbrain.*.*.*	Left Brainstem.Midbrain.*.Gray Matter.Medial Geniculum Body	Left Cerebrum.Sub-lobar.Thalamus.Gray Matter.Ventral Anterior Nucleus	Left Cerebrum.Sub-lobar.Thalamus.Gray Matter.Anterior Nucleus
17	*20*	***10***	***55.2***	***19.9***	***0.7***		***14***				***0.3***				
	21														
7	22	**14.4**	**7.2**	**21.1**	**51.6**		**0.2**		**5.5**						
8	23														
	24														
	25														
	26														
9	27	**7.6**	**59.2**	**25.7**	**1.9**		**2.2**		**3**	**0.2**	**0.2**				
11	28														
	29	23.7			0.2			62.3				13.7			
	30	*31.6*	*14.9*	*29*	*11.8*			*4.5*				*5.5*	*2.6*		
10	*31*	***23.7***			***0.2***			***62.3***				***13.7***			
	32														
	33	*27.7*	*0.3*	*0.6*	*69*		*1.3*					*1.1*			
	34	26.9				5.1	2.4	0.4		64.5				0.6	
	35														
	36														
	37														
	38	24.2	3.4			2.9	0.9	1.9	62.4					2.3	2

Table C.6
The distribution of selected stroke region for each subject(B2 Part)

The range of patients for the neuropsychologic tests	The range of patients during calculating the mean distributions	Right Cerebrum.Sub-lobar.Thalamus.Gray Matter.*	Right Cerebrum.Sub-lobar.Thalamus.Gray Matter.Ventral Posterior Lateral Nucleus	Right Cerebrum.Sub-lobar.Thalamus.Gray Matter.Medial Dorsal Nucleus	Right Cerebrum.Sub-lobar.Thalamus.Gray Matter.Ventral Posterior Medial Nucleus	Right Cerebrum.Sub-lobar.Thalamus.Gray Matter.Mammillary Body	Right Cerebrum.Sub-lobar.Thalamus.Gray Matter.Mammillary Body	Right Cerebrum.Sub-lobar.Thalamus.Gray Matter.Pulvinar	Right Cerebrum.Sub-lobar.Thalamus.Gray Matter.Ventral Lateral Nucleus	Right Cerebrum.Sub-lobar.Thalamus.Gray Matter.Lateral Posterior Nucleus	Right Brainstem.Midbrain.*.*.*	Right Cerebrum.Sub-lobar.Extra-Nuclear.Cerebro-Spinal Fluid.Optic Tract	Right Cerebrum.*.*.*.*	Right Cerebrum.Sub-lobar.Thalamus.Gray Matter.Ventral Anterior Nucleus	Right Cerebrum.Sub-lobar.Thalamus.Gray Matter.Anterior Nucleus
17	*20*														
	21	*11.6*		*86.6*		*1.7*									
7	22														
8	23	**12.5**			**1.3**		**1**	**85.2**							
	24	*44.5*		*0.7*	*6.8*		*16.1*	*32.2*							
	25	*12.5*		*82*		*2.7*		*2*		*0.8*		*0.1*			
	26	*39.6*		*17*					*40.7*				*1*	*1.7*	
9	27														
11	28	**28.7**	**3.9**	**0.7**	**36.3**		**27.4**	**3.1**							
	29	26.2		50.3		15	1.6	5.3		1.2	0.1	0.3			
	30														
10	*31*	*23.9*				*16.7*		*0.9*		*58.1*					***0.4***
	32	*33.7*	*3.7*	*9.7*	3.4		*37.5*	*11.7*	*0.2*						
	33														
	34														
	35	47.2		0.4	0.4		35.7	16.2							
	36	*18*		*74.3*		*0.1*	*7.6*				*0.1*				
	37	72.2		26.2			1.8								
	38														

REFERENCES

1. Sherman, M., and R. W. Guillery, "The role of the thalamus in the flow of information to the cortex," *Phil. Trans. R. Soc. Lond*, no. 357, p. 1695–1708, 2002.

2. Goldstein, M., and C.L.Bolis, eds., *Cerebrovascular Disorders: A Clinical and Research Classification*, World Health Organization, 1978.

3. Donnan, G. A., M. Fisher, M. Macleod, and S. M. Davis, "Stroke," *Lancet*, Vol. 371, pp. 1612–23, May 2008.

4. Henry, J. M. B., J. P. Mohr, M. S. Bennett, and M. Y. Frank, eds., *Stroke-Pathophysiology, Diagnosis and Management*, 2 ed., 1992.

5. Association, A. H., "Heart disease and stroke." `http://www.americanheart.org/downloadable/heart/1240250946756LS-1982HeartandStrokeUpdate.042009.pdf`.

6. Schmahmann, J. D., "Vascular syndromes of the thalamus," *Stroke*, Vol. 34, 2003.

7. Ozel, P., F. I. Uslu, A. D. Duru, and S. B. Erdoğan, "Talamik İnme bölgelerinin bir arayüzle belirlenmesi ve anatomik atlasta eşleştirilmesi," in *Biomedical Engineering Meeting*, pp. 1–3, April 2010.

8. Steinke, W. S., R. L. Sacco, J. P. Mohr, M. A. Foulkes, and T. K. Tatemichi, "Thalamic stroke: presentation and prognosis of infarcts and hemorrhages," *Arch Neurol.*, no. 49, pp. 703–710, 1992.

9. Fisher, C., "The pathologic and clinical aspects of thalamic hemorrhage," *Trans Am Neurol Assoc.*, no. 84, pp. 56–59, 1959.

10. Mohr, J. P., W. C. Watters, and G. W. Duncan, "Thalamic hemorrhage and aphasia," *Brain Lang*, no. 2(1), pp. 3–17, 1975.

11. Kumral, E., T. Kocaer, N. O. Ertübey, and K. Kumaral, "Thalamic hemorrhage-a prospective study of 100 patients," *Stroke*, no. 26, pp. 964–970, 1995.

12. Ocariz, M. M., "Risk factors and clinical course for infarcts and hemorrhages," *Stroke*, no. 27, pp. 1530–1536, 1996.

13. Uslu, F. I., *Talamik Infractlarda Lokalizasyon,Elektrosefalografi ve Neropsikolojik Bulguların Korelasyonu.* PhD thesis, Istanbul Universitesi Istanbul Tıp Fakültesi Noroloji Anabilim Dalı, 2010.

14. Greenstein, B., and A. Greenstein, eds., *Color Atlas of Neuroscience*, Theime, 2000.

15. Brazis, P. W., C. M. Jose, and B. Jose, "The anatomic localization of lesions İn the thalamus," in *Localization İn Clinical Neurology*, pp. 399–420.

16. Graff-Radford, N. R., J. E. Paul, R. D. A. R. Damasio, and Y. Thorn, "Nonhemorrhagic infarction of the thalamus: Behavioral, anatomic, and physiologic correlates," *Neurology*, no. 34, pp. 14–23, 1984.

17. Association, A. H., "Diagnose." `http://www.strokeassociation.org/STROKEORG/AboutStroke/Diagnosis/Diagnosis_UCM_310890_Article.jsp`.

18. Warach, S., J. Gaa, B. Siewert, P. Wielopolski, and R. R. Edelman, "Acute human stroke studied by whole brain echo planar diffusion-weighted magnetic resonance imaging," *Ann Neurol.*, pp. 231–41, Feb 1995.

19. Rovaris, M., M. Inglese, B. Viti, G. Ciboddo, S. Gerevini, R. Capra, and M. Filippi, "The contribution of fast-flair mri for lesion detection in the brain of patients with systemic autoimmune diseases," *J Neurol*, no. 247, pp. 29–33, 2000.

20. Jordan, K. G., "Emergency eeg and continuous eeg monitoring in acute ischemic stroke," *Journal of Clinical Neurophysiology*, Vol. 21, pp. 56–59, October 2004.

21. Courville, C. B., "Etiology and pathogenesis of laminar cortical necrosisits significance in evaluation of uniform cortical atrophies of early life," *Arch Neurol Psychiatry*, no. 79, pp. 7–30, 1958.

22. Hartings, J. A., A. J. Williams, and F. C. Tortella, "Occurrence of nonconvulsive seizures, periodic epileptiform discharges, and intermittent rhythmic delta activity in rat focal ischemia," *Exp Neurol*, no. 84, pp. 139–49, 2003.

23. Sundt, T. M., F. W. Sharbrough, D. G. Piepgras, T. P. Kearns, J. M. J. Messick, and W. M. OFallon, "Correlation of cerebral blood flow and electroencephalographic changes during carotid endarterectomy with results of surgery and hemodynamics of cerebral ischemia.," *Mayo Clin Proc*, no. 56, pp. 533–43, 1981.

24. Bruce, F., H. S. David, and B. Evelina, "Neurotechnique automated labeling of neuroanatomical structures in the human brain," *Neuron*, Vol. 33, pp. 341–355, January 2002.

25. Talairach, J., M. David, P. Tournoux, H. Corredor, and T. Kvasina, "Atlas d'anatomie stereotaxique des noyaux gris centraux," 1957.

26. Schaltenbrand, G., and W. Bailey, "Introduction to stereotaxis with an atlas of the human brain," no. 84, pp. 56–59, 1959.

27. Bertrand, G., A. Olivier, and C. J. Thompson, "Computer display of stereotaxic brain maps and probe tracts," *Acta Neurochir*, no. 21, pp. 235–243, 1974.

28. Talairach, J., and P. Tournoux, "Co-planar stereotactic atlas of the human brain," 1988.

29. Fox, P. T., S. Mikiten, G. Davis, and J. L. Lancaster, "Brainmap: A database of human functional brain mapping.," 1994.

30. Lancaster, J. L., M. G. Woldorff, and L. M. Parsons, "Automated talairach atlas labels for functional brain mapping," *Hum Brain Mapp*, no. 10, pp. 120–31, 2000.

31. Lancaster, J. L., L. H. Rainey, J. L. Summerlin, C. S. Freitas, P. T. Fox, A. E. Evans, A. W. Toga, and J.C.Mazziotta, "Automated labeling of the human brain: A preliminary report on the development and evaluation of a forward-transform method," *Hum Brain Maping*, no. 5, pp. 238–242, 1997.

32. Toga, A. W., and P. M. Thompson, "Maps of the brain," *Anat Rec*, no. 265, pp. 37–53, 2001.

33. Kim, J. S., D. S. Lee, and B. T. Lee, "Probabilistic anatomical labeling of brain structures using statistical probabilistic anatomical maps," *Korean J Nucl Med*, no. 36, pp. 317–24, 2002.

34. Lee, J. S., D. F. Wong, Y. Zhou, and R. Hoehn, "Localization of neural substrates of worry using h 215o pet and probabilistic brain atlas," *J Cereb Blood Flow Metab*, no. 23(S1), p. 713, 2003.

35. Nowinski, W. L., A. Fang, B. T. Nguyen, J. K. Raphel, L. Jagannathan, R. Raghavan, R. N. Bryan, and G.Miller, "Multiple brain atlas database and atlas-based neuroimaging system," *Comput. Aided Surg.*, no. 2(1), pp. 42–66, 1997.

36. Nowinski, W. L., and A. Thirunavuukarasuu, "Atlas-assisted localization analysis of functional images.," *Med. Image Anal*, no. 5(3), pp. 207–220, 1959.

37. Nowinski, W. L., and D. Belov, "The cerefy neuroradiology atlas: a talairach–tournoux atlas-based tool for analysis of neuroimages available over the internet.," *Neuroimage*, no. 20, pp. 50–57, 2003.

38. LCollins, D., P. Neelin, T. M. Peters, and A. C. Evans, "Automatic 3d intersubject registration of mr volumetric data in standardized talairach space.," *Comput. Assist. Tomogr.*, no. 18, pp. 192–205, 1994.

39. Evans, A. C., S. Marrett, P. Neelin, L. Collins, K. Worsley, W. Dai, S. Milot, E. Meyer, and D. Bub, "Anatomical mapping of functional activation in stereotactic coordinate space.," *NeuroImage*, no. 1, pp. 43–53, 1992.

40. Brett, M., I. S. Johnsrude, and A. M. Owen, "The problem of functional localization in the human brain.," *Neurosci.*, no. 3, pp. 243–249, 2002.

41. Talairach, J., and P. Tournoux, "Referentially oriented cerebral mri anatomy: Atlas of stereotaxic anatomical correlations for gray and white matter," *Trans Am Neurol Assoc.*, 1993.

42. Ono, M., and S. Kubik, eds., *Atlas of the Cerebral Sulci*, Theime, 1990.

43. Bohland, J. W., H. Bokil, C. B. Allen, and P. P. Mitra, "The brain atlas concordance problem: Quantitative comparison of anatomical parcellations," *PLoS ONE*, no. 4(9), 2009.

44. Eickhoff, S. B., K. E. Stephan, H. Mohlberg, C. Grefkes, G. R. F. GR, K. Amunts, and K. Zilles, "A new spm toolbox for combining probabilistic cytoarchitectonic maps and functional imaging data," *Neuroimage*, no. 25(4), pp. 1325–35, 2005.

45. Eickhoff, S. B., S. Heim, K. Zilles, and K. Amounts, "Testing anatomically specified hypotheses in functional imaging using cytoarchitectonic maps," *Neuroimage*, no. 32(2), pp. 570–582, 2006.

46. Eickhoff, S. B., T. Paus, S. Caspers, M. H. Grosbras, and A. C. Evans, "Assignment of functional activations to probabilistic cytoarchitectonic areas revisited," *Neuroimage*, no. 36(3), pp. 511–521, 2007.

47. Diedrichsen, J., J. H. Balster, E. Cussans, and N. Ramnani, "A probabilistic mr atlas of the human cerebellum," *Neuroimage*, 2009.

48. Shattuck, D. W., M. Mirza, V. Adisetiyo, C. Hojatkashani, G. Salamon, K. L. Narr, R. A. Poldrack, R. M. Bilder, and A. W. Toga, "Construction of a 3d probabilistic atlas of human brain structures," *Neuroimage*, no. 39(3), pp. 1064–1080, 2008.

49. Rohlfing, T., N. M. Zahr, E. V. Sullivan, and A. Pfefferbaum, "The sri24 multichannel atlas of normal adult human brain structure," *Hum Brain Mapp*, no. 31, pp. 798–819, 2010.

50. J.Behrens, T. E., H. J. Berg, M. W. Woolrich, S. M. Smith, C. A. M. Wheeler, and P. A. Baulbay, "Non-invasive mapping of connections between human thalamus and cortex using diffusion imaging," *Nature Neuroscience*, no. 6(7), pp. 750–757, 2003.

51. Behrens, T. E. J., H. Berg, M. W. Woolrich, S. M. Smith, J. M. Brady, and S. Clare, "Characterisation and propagation of uncertainty in diffusion weighted mr imaging," *Magnetic Resonance in Medicine*, no. 50, pp. 1077–1088, 2003.

52. Behrens, T., H. Johansen-Berg, and D. Flitney, "Thalamic Connectivity Atlas, howpublished=`http://www.fmrib.ox.ac.uk/connect/`."

53. Nielsen, F. A., and L. K. Hansen, "Experiences with matlab and vrml in functional neuroimaging visualizations," *Trans Am Neurol Assoc.*, no. 84, pp. 56–59, 2000.

54. Nielsen, F. A., "Mass meta-analysis in talairach space," *In Advances in Neural Information Processing Systems*, no. 17, pp. 985–992.

55. Nielsen, F. A., "Data mining a functional neuroimaging database for functional segregation in brain regions," 2006.

56. Nielsen, F. A., "The brede database: a small database for functional neuroimaging," *Neuroimage*, no. 19.

57. Nielsen, F. A., "Visualizing data mining results with the brede tools," *Frontiers in Neuroinformatics*, Vol. 3, July 2009.

58. Maldjian, J. A., P. J. Laurienti, and J. H. Burdette, "Precentral gyrus discrepancy in electronic versions of the talairach atlas," *NeuroImage*, no. 21, pp. 450–455, 2004.

59. Maldjian, J. A., P. J. Laurienti, and R. A. Kraft, "Burdette jh. an automated method for neuroanatomic and cytoarchitectonic atlas-based interrogation of fmri data sets," *Neuroimage*, no. 19, pp. 1233–1239, 2003.

60. Klein, A., and J. Hirsch, "Mindboggle: a scatterbrained approach to automate brain labeling," *Neuroimahe*, no. 24, pp. 261–280, 2005.

61. Nowinski, W. L., and A. Thirunavuukarasuu, "A locus-driven mechanism for rapid and automated atlas-assisted analysis of functional images by using the brain atlas for functional imaging," *Neurosurg Focus*, no. 15(1), 2003.

62. Gardner, D., and G. M. Shepherd, "A gateway to the future of neuroinformatics," *Neuroinformatics*, no. 2, pp. 271–274, 2004.

63. Gardner, D., H. Akil, G. Ascoli, D. M. Bowden, W. Bug, D. E. Donohoe, D. B. G. D Goldberg, J. S. Grethe, A. Gupta, M. Halavi, D. N. Kennedy, L. Marenco, M. E. Martone, P. L. Miller, H. M. Müller, A. Robert, G. M. Shepherd, P. W. Sternberg, D. C. V.Essen, and R. W. Williams, "The neuroscience information framework: a dataand knowledge environment for neuroscience," *Neuroinformatics*, no. 6, pp. 149–160, 2008.

64. Buccigrossi, R., M. Ellisman, J. Grethe, C. Haselgrove, D. Kennedy, M. Martone, N. Preuss, M. Sullivan, and K. Wagner, "The neuroimaginginformatics tools andresources clearinghouse," *In 14th Annual Meeting of theOrganization for Human BrainMapping*, p. 319.

65. Dinov, I. D., D. Rubin, W. Lorensen, J. Dugan, S. Murphy, B. Kirschner, M. Sherman, A. Floratos, D. Kennedy, H. V. Jagadish, J. Schmidt, B. Athey, A. Califano, M. Musen, R. Kikinis, I. KohaneI, S. Delp, D. S. Parker, and A. W. Toga, "itools: a framework for classification, categorization and integrationof computational biology resources," *PLoS ONE*, 2008.

66. Nielsen, F. A., "Brede wiki: neuroscience data structured in a wiki. in proceedings of the fourth workshop on semantic wikis," *The Semantic Wiki Web*, no. 84, pp. 129–133, 2009.

67. Cocosco, C. A., and A. C. Evans, "Java internet viewer: a www tool for remote 3d medical image data visualization and comparison. in proceedings of the 4th international conference on medical image computing and computer-assisted intervention," Vol. 2208, pp. 1415–1416, 2001.

68. Lee, J. T., K. R. Munch, J. V. Carlis, and J. V. Pardo, "Internet image viewer (iiv)," *BMC Med. Imaging*, 2008.

69. Moore, E. B., A. V. Poliakov, P. Lincoln, and J. F. Brinkley, "Mindseer: a portable and extensible tool for visualization of structural and functional neuroimaging data.," *BMC Bioinformatics*, no. 8, p. 389, 2007.

70. Gustafson, C., W. J. Bug, and J. Nissanov, "Neuroterrain – a client–server system for browsing 3d biomedical image data," *BMC Bioinformatics*, no. 8, p. 40, 2007.

71. Laird, A. R., J. L. Lancaster, and P. T. Fox, "Brainmap: the social evolution of a human brain mapping database," *Neuroinformatics*, no. 3, pp. 65–78, 2005.

72. Kennedy, D. N., C. Haselgrove, and S. McInerney, "Mribased morphometric analysis of typical and atypical brain development.," *Ment. Retard. Dev. Disabil. Res. Rev.*, pp. 155–160, May.

73. Dombeck, M., "Neuropsychological tests." `http://www.mentalhelp.net/poc/view_doc.php?type=doc&id=8220&cn=18`.

74. Folstein, M. F., S. E. Folstei, and P. R. McHugh, "Mini-mental state". a practical method for grading the cognitive state of patients for the clinician," *Journal of psychiatric research*, Vol. 12, no. 3, pp. 189–98, 1975.

75. Mungas, D., "In-office mental status testing: a practical guide," *Geriatrics*, Vol. 46, pp. 54–8,63–66, July 1991.

76. Crum, R. M., J. C. Anthony, S. S. Bassett, and M. F. Folstein, "Population-based norms for the mini-mental state examination by age and educational level," *JAMA*, Vol. 269, pp. 2386–91, May 1993.

77. Kertesz, A., W. Davidson, and H. Fox, "Frontal behavioral inventory: diagnostic criteria for frontal lobe dementia," *Can J Neurol Sci.*, Vol. 24, pp. 29–36, Feb 1997.

78. Kertesz, A., W. Davidson, and H. Fox, "The frontal behavioral inventory in the differential diagnosis of frontotemporal dementia," *J Int Neuropsychol Soc*, Vol. 6, pp. 460–8, May 2000.

79. Tegin, B., *Depresyonda bilişsel bozukluklar Beck modeline göre bir inceleme*. PhD thesis, Hacettepe Universitesi Psikoloji Bölümü, 1980.

80. Hisli, N., "Beck depresyon envanteri'nın Üniversite öğrencileri için geçerliği, güvenirliği," *Psikoloji Dergisi,*, Vol. 7, pp. 3–13, May 1988.

81. *Depression: Causes and Treatment*, University of Pennsylvania Press, 2006.

82. Steer, R. A., R. Ball, W. F. Ranieri, and A. T. Beck, "Dimensions of the beck depression inventory-ii in clinically depressed outpatients," *Journal of clinical psychology*, Vol. 55, pp. 117–28, January 1999.

83. Brown, L. G., "A survey of image registration techniques," *ACM Computing Surveys (CSUR) archive*, Vol. 24, pp. 325–376, December 1992.

84. Fitzpatrick, J. M., D. L. G. Hill, and C. R. Maurer, "Image registration." `http://tango.andrew.cmu.edu/~gustavor/42431-intro-bioimaging/readings/ch8.pdf`.

85. Ashburner, J., and K. J. Friston, "Rigid body registration." `http://www.fil.ion.ucl.ac.uk/spm/doc/books/hbf2/pdfs/Ch2.pdf`.

86. Ashburner, J., and K. J. Friston, "Multimodal image coregistration and partitioning-a unified framework," *Neuroimage*, no. 6, pp. 209–217, 1997.

87. Ashburner, J., and K. J. Friston, "Spatial normalization using basis functions." `http://www.fil.ion.ucl.ac.uk/spm/doc/books/hbf2/pdfs/Ch3.pdf`.

88. Freitas, C. S., J. L. Summerlin, J. L. Lancaster, and P. T. Fox, "The pathologic and clinical aspects of thalamic hemorrhage," *Soc Neurosci*, 1996.

89. Brett, M., "The mni brain and the talairach atlas." `http://imaging.mrc-cbu.cam.ac.uk/imaging/MniTalairach`.

90. Lancaster, J. L., D. T. Gutierrez, and M. Martinez, "Bias between mni and talairach coordinates analyzed using the icbm 152 brain template.," *Hum Brain Mapp*, no. 28, pp. 1194–205.

91. Fox, P., and A. Laird, "Converting between mni and talairach spaces." `http://brainmap.org/icbm2tal/`.

92. Machin, D., M. Campbell, P. Fayers, and A. Pinol, *Sample size tables for clinical studies*, 2nd ed., 1997.

93. Kim, J., B. A. ans Sunil Patel, and J. Whyte, "Spatial normalization of injured brains for neuroimaging research: An illustrative introduction of available options," Moss Rehabilitation Research Institue, 2008.

94. Nachev, P., E. Coulthard, H. R. Jager, C. Kennard, and M. Husain, "Enantiomorphic normalization of focally lesioned brains," *Neuroimage*, no. 39(3), pp. 1215–1226, 2005.

95. Ashburner, J., and K. J. Friston., "Unified segmentation," *Neuroimage*, no. 26, pp. 839–851, 2005.

96. Nowinski, W. L., "Electronic brain atlases: features and applications," in *3D Image Processing: Techniques and Clinical Applications*, pp. 79–83, 2002.

97. Rogelj, P., S. Kovacic, and J. Gee, "Validation of a nonrigid registration algorithm for multimodal data," pp. 299–307, 2002.

98. Grachev, I. D., D. Berdichevsky, S. L. Rauch, S. Heckers, D. N. Kennedy, V. S. Caviness, and N. M. Alpert, "A method for assessing the accuracy of intersubject registration of the human brain using anatomic landmarks," *NeuroImage*, no. 9, pp. 250–268.

99. Dinov, I. D., and D. W. L. Sumners, "Applications of frequency dependent wavelet shrinkage to analyzing quality of image registration," pp. 367–384, 2001.

100. Robbins, S., A. C. Evans, D. L. Collins, and S. Whitesides, "Tuning and comparing spatial normalization methods," *Med Image Anal*, no. 8, pp. 311–323, 2004.